Chapter 2

LITERATURE REVIEW

2.1 General

Underground mining most often involves in leaving of ore portions in the form of pillars, and they serve as essential structural columns (Deng et al., Brady and Brown 2003; 2003; Zhou et al., 2011). Pillars are one of the important structural units used in underground mines to ensure safety. Their functions are to ensure global stability by equipping a safer environment where excavation works progress and supporting the weight of load exerting on the pillar strata (Ghasemi et al., 2014; Liang et al., 2019). As the depth of cover increases, there is an increase in the ambient stress resulting in frequent pillar failure. As a result, pillar design and pillar stability are important aspects as well as complicated but inherent issues in the extraction of the ores relating to ground control and rock mechanics. Because of their great importance in the safer and cost-effective extraction of underground ores over the last few decades, several authors have reported a wealth of valuable results on a variety of topics. It has made commendable efforts in terms of designing the pillars and outlines used in rocks. Unstable pillars can lead to large-scale catastrophic collapses and significantly decrease worker safety (Wang et al., 2008). When a pillar fails, the load on the adjacent pillars increases due to which the strength of adjacent pillars decreases, causing them to fail. In such a scenario, sudden and collateral damage can occur (Zhou et al., 2018). Furthermore, as mining depth increases, stress on the pillars increases, and the pillar instability accidents become even more frequent (Peng et al., 2019; Luoet al., 2019). As a result, assessing pillar stability has been a prerequisite to accomplishing secure and convenient mining.

Conventionally there are three methods were used to evaluate pillar stability in underground mines. The first is the approach based on the safety factor. The safety factor denotes the pillar's resistance to stress (González et al. 2006). This method should be used to determine three components: pillar strength, pillar stress, and safety limit. Many empirical methods for calculating pillar strength are proposed, for example, the linear shape effect, power shape effect, size effect, and Hoek–Brown formulas (Zhou et al. 2015) which have been further explained in this chapter. The main approaches for determining pillar stress are tributary area theory and numerical modeling techniques (Lunder,1994). The pillar strength and pillar stress are two essential factors used to calculate the safety factor. A more eminent value of safety factor indicates a more stable pillar. In theory, the safety factor threshold is set to one. For stable pillars the safety factor is greater than one, otherwise, it is considered to be unstable (Cauvin et al. 2009). In practice, the safety threshold has been usually greater than one. As it is known that utilization of safety factor method are concise and simple to use but still the determination of pillar strength formula and safety threshold are not done at large scale. The second technique is a numerical simulation in which complicated boundary conditions and rock mass properties can be used to determine pillar stability. In modern days numerical simulations are widely used. Mortazavi et al. (2009) investigated the non-linear behavior of rock pillars and their failure process and used the fast Lagrangian analysis of continua (FLAC) method in addition to its FLAC3D model used by Shnorhokian et al. (2015) to evaluate pillar stability in different mining sequence scenarios. The work of Elmo and Stead (2015) investigated the failure characteristics of naturally fractured pillars using the finite element method (FEM) and the discrete element method (DEM). Li et al. (2013) assessed pillar stability

using rock failure process analysis (RFPA) under coupled thermo-hydrologic-mechanical conditions. Moreover, the boundary element method (BEM) was applied by Jaiswal et al. (2004) to simulate asymmetry in induced stresses over pillars, and Li et al. (2019) used the finite-discrete element method (FDEM) to investigate the mechanical behaviour and failure mechanisms of the pillar. Furthermore, some researchers studied pillar stability using a combination of numerical simulation and other mathematical models. Deng et al. (2003optimizeded pillar design using FEM, neural networks, and reliability analysis, while Griffiths et al. (2002) examined pillar failure probability using random field theory, an elastoplastic finite element algorithm, and a Monte-Carlo approach. The complex failure behaviors of pillars can be modeled using numerical simulation techniques, and the failure process and range can be determined. However, the determination of model input and consecutive equations is difficult because of the anisotropy and non-linear characteristics of the rock mass. As a result, a limited accuracy was observed in the result by this method.

The machine learning (ML) algorithm is the third. An amount of large data has been managed to help in emergencies events and in natural disasters (Amato et.al. 2019). The accumulation of pillar stability cases enables researchers to create advanced predictive models using machine learning algorithms to overcome pillar stability problems. Tawadrous and Katsabanis (2007) investigated the stability of surface crown pillars using artificial neural networks (ANN). Wattimena (2014) proposed multinomial logistic regression (MLR) for predicting pillar stability. To predict pillar stability, Ding et al. (2018) used a stochastic gradient boosting (SGB) model, which outperformed the random forest (RF), support vector machine (SVM), and multilayer perceptron neural networks (MPNN). Ghasemi et al. (2017) developed two-pillar stability graphs with

acceptable prediction accuracy using the J48 and SVM algorithms. Zhou et al. (2009) compared the performance of six supervised learning methods in predicting pillar stability and discovered that SVM and RF performance were better than the other deployed tools. Stochastic gradient boosting (SGB) model has been proposed by H Ding et al. (2018) in order to predicting pillar stability. Two new models (random tree and C4.5 decision tree algorithms) are proposed to predict pillar stability for underground coal and stone mines (M Ahmed et al. 2020).

Although these ML algorithms can help in predicting pillar stability to some extent, none of them can be applied to all engineering conditions. Currently, there is no industry-wide consensus on a uniform algorithm. When compared to traditional safety factor and numerical simulation methods, the ML approach can uncover hidden relationships between variables and handle nonlinear problems effectively. As a result, it appears to be a promising method for predicting pillar stability.

In addition to the ML algorithms mentioned above, the gradient boosting decision tree (GBDT) method has demonstrated excellent prediction performance in a variety of fields (Sun et al. 2020; Lombardo et al. 2015; Tama et al. 2019). It is one of the ensemble learning algorithms that use the boosting approach to combine multiple decision trees (DTs) into a strong classifier (Sachdeva et al.2018). DTs is an ML method that uses a tree-like structure to deal with various types of data and trace each path in the prediction of the results (Kotsiantis,2013). DTs, on the other hand, are easily overfit and sensitive to dataset noise. Because the errors of the DTs are compensated for by each other, the overall prediction performance of the GBDT improves with the integration of DTs. Extreme gradient boosting (XGBoost) (Chen et al. 2016) and light gradient boosting machine (LightGBM) (Ke et al. 2016) have recently been proposed

within the framework of GBDT, extreme gradient boosting (XGBoost) (Chen et al. 2016)) and light gradient boosting machine (LightGBM) (Ke et al. 2016) have been proposed recently.They have also received widespread attention as a result of their outstanding performances. Surprisingly, these three algorithms perform well on small datasets. Overfitting, which occurs when a model fits the existing data too precisely but fails to predict future data reliably, can also be avoided to some extent. To the best of our knowledge, however, the GBDT, XGBoost, and LightGBM algorithms have never been used to predict pillar stability in hard rock mines.

2.2 Pillar Mechanics

Recently, it has been found that the pillar width-to-pillar height ratio has been determined the mechanics of the behavior during its loading. Hence, this ratio was the single most important parameter in pillar design (Salamon,2003). Pillar failure mechanics was largely influenced by the size of the pillars and the shape of the pillars. Therefore, attempts were being made for the quantification of the influence of w/h. Currently, the broad variation in coal pillar mechanics has been accepted for the slender and squat pillars.

A proper understanding of the behavior of the pillar has the potential of reducing pillar dimensions without sacrificing safety and increasing mineable coal (Thin et al., 2003). Mark (2006) observed that pillar shape influenced the strength of the coal pillars. Mark (1999) had identified three categories of pillar behavior and failure modes corresponding to approximate ranges of pillar width-to-pillar height ratios.

Slender pillars The w/h ratios of slender pillars were less than four. When the load on the pillars exceeds their maximum capacity, they completely failed, the overlying strata collapse. When a significant number of slender pillars were used over a large area, a single pillar failure could trigger a cascade, leading to a massive collapse accompanied by an impactful air blast.

Intermediate pillars The w/h ratios of intermediate pillars ranged between four and eight. On failure, these pillars did not drop their entire weight of overburden in order to accept any further deformation. Instead, they deformed until the overburden's flexure transferred some of their weight away from them. The end result was usually a nonviolent "squeeze" that lasted hours, days, or even weeks. Large roof-to-floor closures associated with squeezes could create destructive ground conditions and equipment entrapment.

Squat pillars Squat pillars with w/h ratios greater than ten may be capable of carrying a massive load, hence they can bear maximum stress.This means they may never shed load and become much more deformable once they fail. The squat pillars' strength can vary greatly depending on the presence of soft parting, weak roof or floor interfaces, and other geological factors. This model of pillar mechanics is based on the recent convergence and similarities in the findings of empirical studies and numerical methods.

The complete stress-strain curve in uniaxial compression obtained in-situ for a square coal specimen of 1.4 m width is depicted in Figure 2.1. (Bieniaweski and Heerden, 1975). Figure 2.2 depicts the results of underground tests on coal pillars (Wagner, 1974). He measured the stress distribution inside the pillar and concluded that

the pillar's edge could resist relatively little stress. However, this section of the pillar provided lateral confinement to the core, increasing the strength of the pillars' core. These tests also revealed that rectangular cross-section pillars were up to 40% stronger than square pillars of the same width and height due to the square pillars' relatively smaller perimeter (Wagner,1974; Bieniawski,1975).

The load-deformation curves of the underground pillars with varying pillar width-to-pillar height ratios are shown in Figure 2.3. Here the mean stress values are plotted as the function of the mean value of pillar compression. The curves are presented for the integer values of width-to-height ratios from one to eight. All curves show ascending and descending branches. The peak values which separate the branches represent the strength of the pillars. As the ratio to pillar width-to-pillar height increases, pillar strength also increases remarkably. The strain-softening or the descending branches deform smoothly up to about a pillar width-to-pillar height ratio of three. All descending curves corresponding to ratios four or higher show a pronounced drop in resistance (Salamon,2003).

Das (1986) published data from a laboratory study of pillars with varying pillar width-to-pillar height ratios, as shown in Figure 2.4. It depicts the post-failure behavior and residual strength of coal pillars as their shape changes.

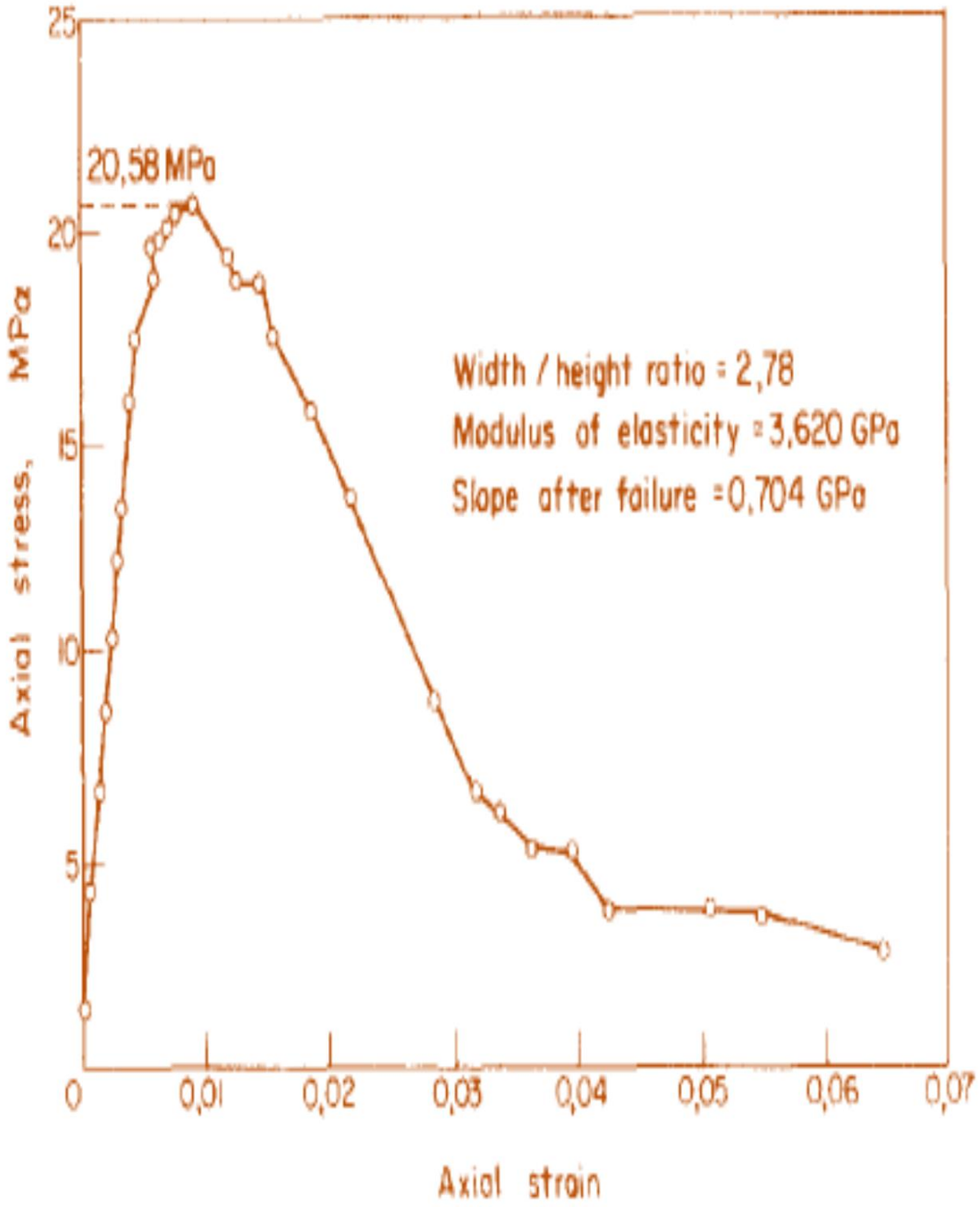

Figure 2.1. In-situ stress-strain curve of coal specimen(square shaped) with a width of 1.4m in uniaxial compression (Beiniawski and van Heerden,1975).

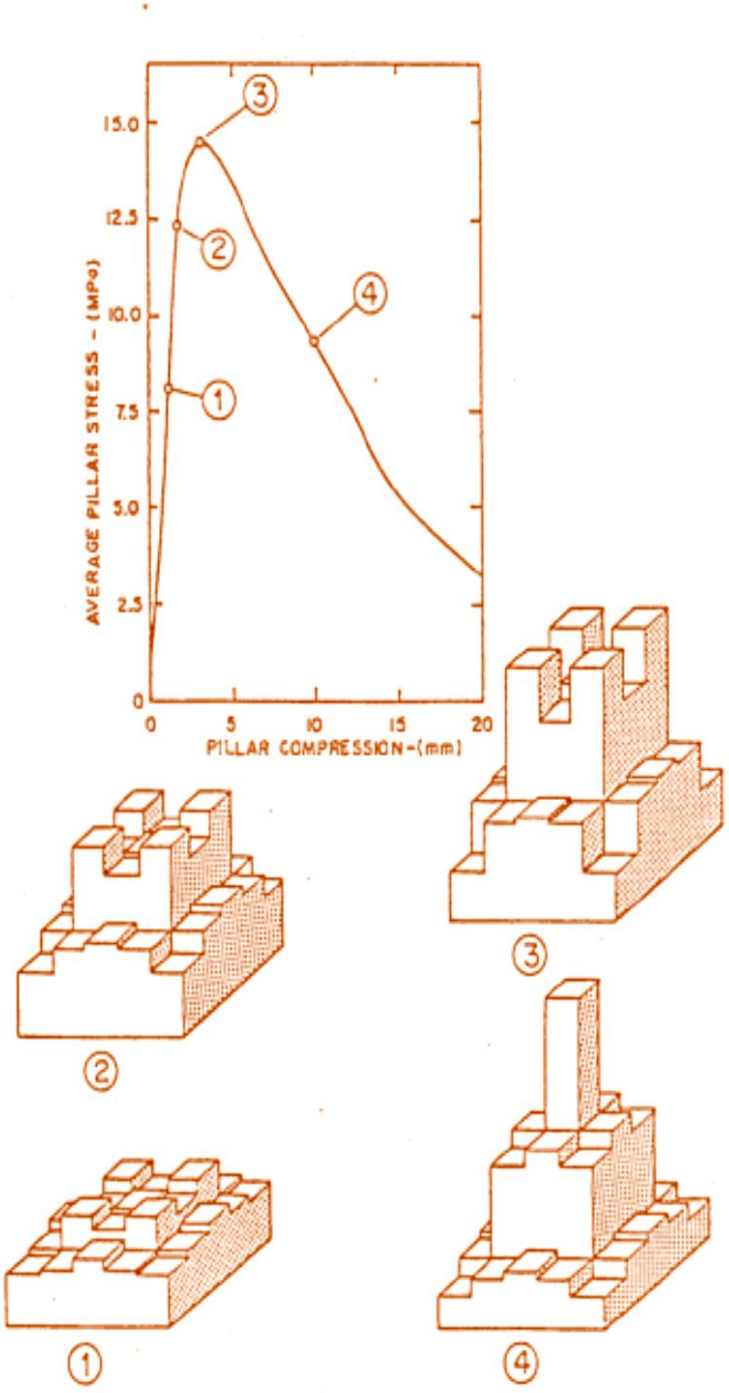

Figure 2.2: Stress profiles at different stages of coal pillar compression for w/h =2. (Wagner, 1974).

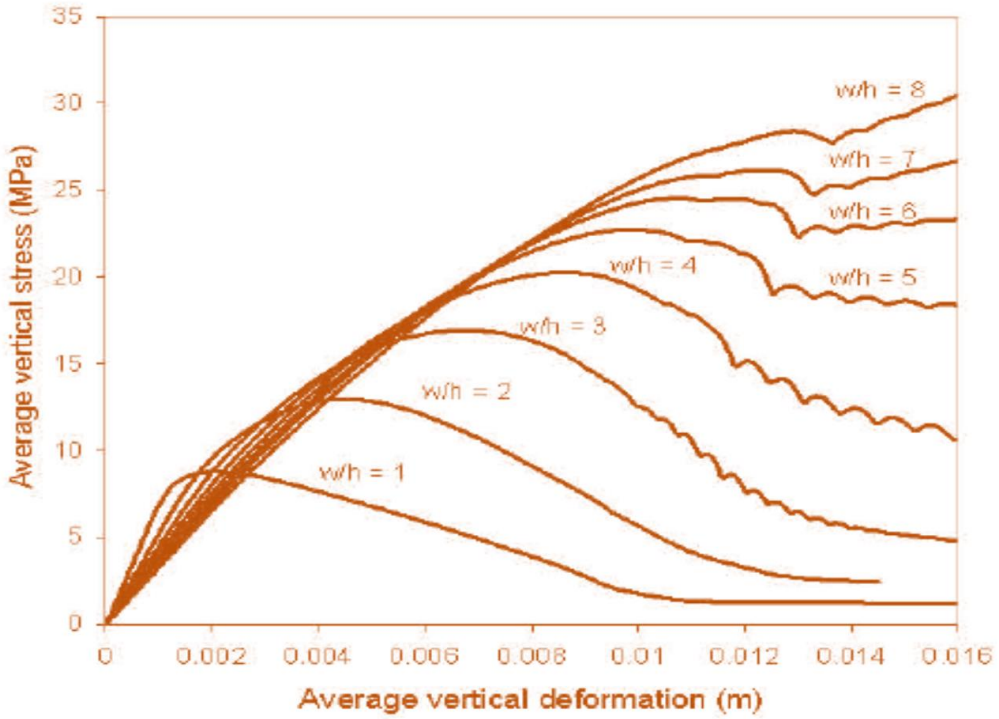

Figure 2.3. Average pillar stress-deformation relationship using strain-softening criterion (Salamon,2003)

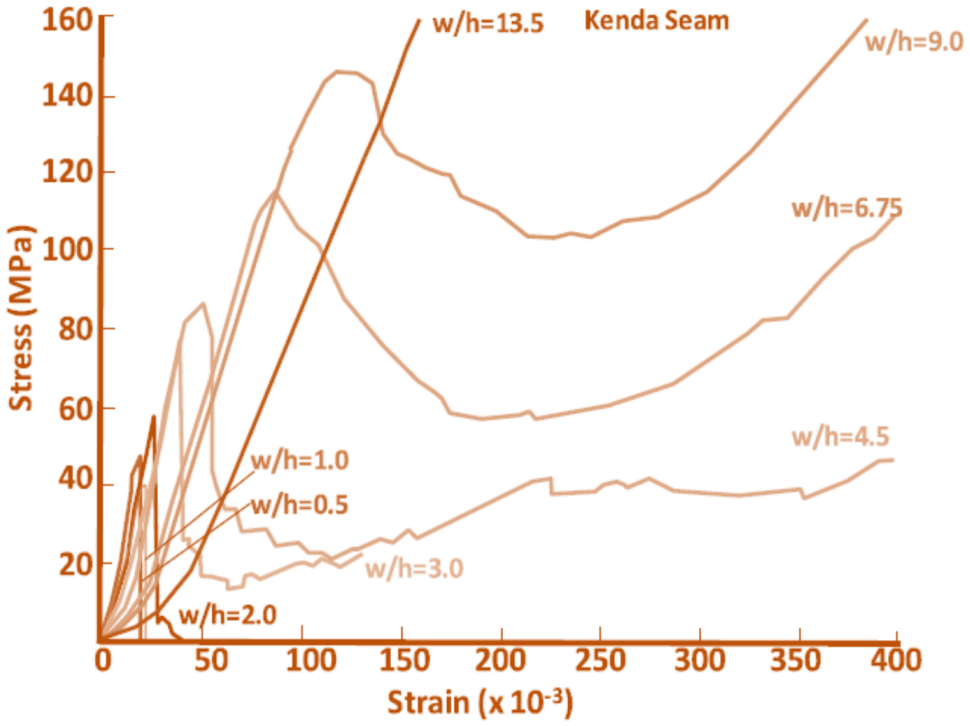

Figure 2.4 The variation of coal pillar with w/h ratio (Das,1986).

2.3 Factor related to pillar stability

Table 2.1 shows the five-category classification of pillar failure as suggested by Krauland & Soder (1987). The factors contributing to pillar stability and pillar strength are discussed in the following section:

Table 2.1: The classification of pillar failure.

Classification of Pillar Stability	Conditions related to pillars
0	There are no fractures.
1	Mild spalling and a very small amount of fractures.
2	A little number of fractures near the surface, as well as a definite amount of spalling
3	A measurable amount of fractures in the center of pillars.
4	A few amounts of fracture has been seen through the center of pillars, which may parallel or diagonal to pillar walls showing the emergence of an hourglass shape.
5	Well noted amount of fracture in pillars with major block falling mean totally disintegrates. Alternatively the , center party is totally crushed with the emergence of an hourglass shape.

2.3.1 Rock Strength

The UCS of the intact pillar material is one of the dominating factors on mine pillar strength. This information can be obtained using various tests like the hammer test, point load index and small-scale laboratory sample. However, such pillar strength assessments completely ignore the induced structural defects and associated variability in the strength of the rock mass. The UCS is the most significant value, which represents the strength of rock mass in several mining situations. The true UCS value cannot be determined accurately by unconfined strength. There are several methods, such as the strength correction factor, also known as the size effect formula are commonly used to translate laboratory values of intact rock strength.

2.3.2 Pillar Stress

When the pillar load/stress dominants the pillar strength, failure of pillars occurs . This is visible as pillar material rupturing and shear failure. To assess pillar strength, an estimate of pillar stress must be obtained and compared to the determined pillar strength. As a result, pillar stress is an important factor in determining pillar strength.

2.3.3 Pillar Shape

According to the researchers, pillar shape has very much significance in estimating the strength of the pillars. It is widely accepted the pillar strength is weaker for the slender pillars. Figure 2.5 depicts the impact of pillar shape on pillar strength (Hoek and Brown 1980). In all cases, as w/h ratio increases, the pillar strength increases.

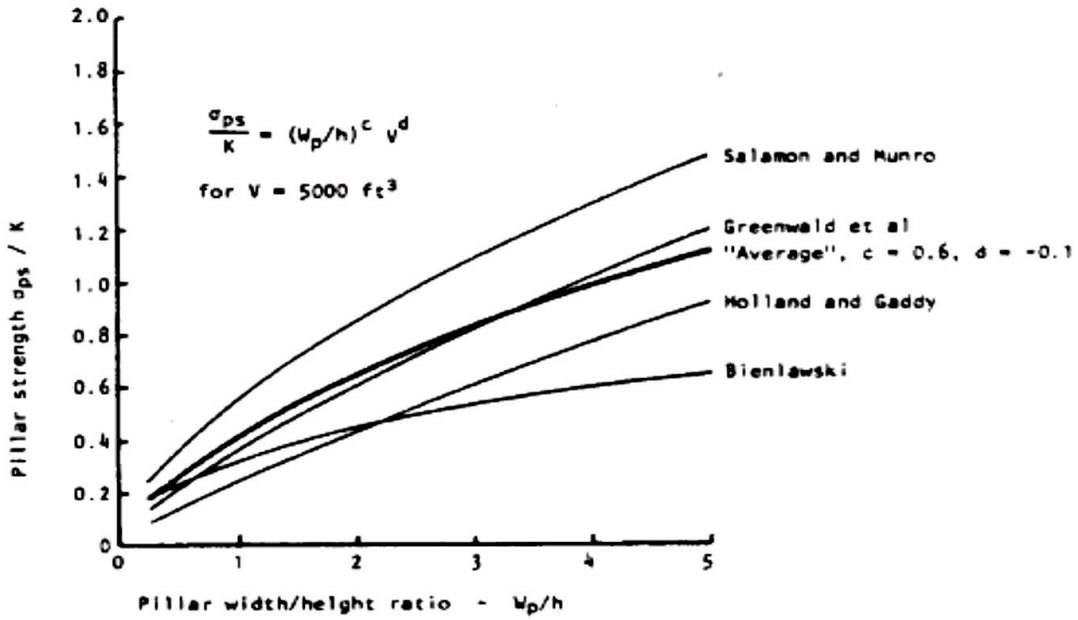

Figure 2.5. Relationship between pillar shape and pillar strength (Hoek and Brown,1980).

2.3.4 Pillar Volume

Generally, it is assumed that the larger the volume of pillars, there will be the more number of structural defaults which denotes the lesser amount of pillar strength for the given

w/h ratio. This relationship, however, has an upper limit. The effects of the pillar volume researched on the pillar strength has been shown by different researchers has been depicted in Figure 2.6. Figure 2.7 depicts a curve relating to strength samples to sample size for numerous sized specimens. The curves display that as the sample size reaches a critical limit, the strength loss becomes constant. Figure 2.8 illustrates the influence of sample size on the strength testing of small-scale intact samples. (Kostak,1971).

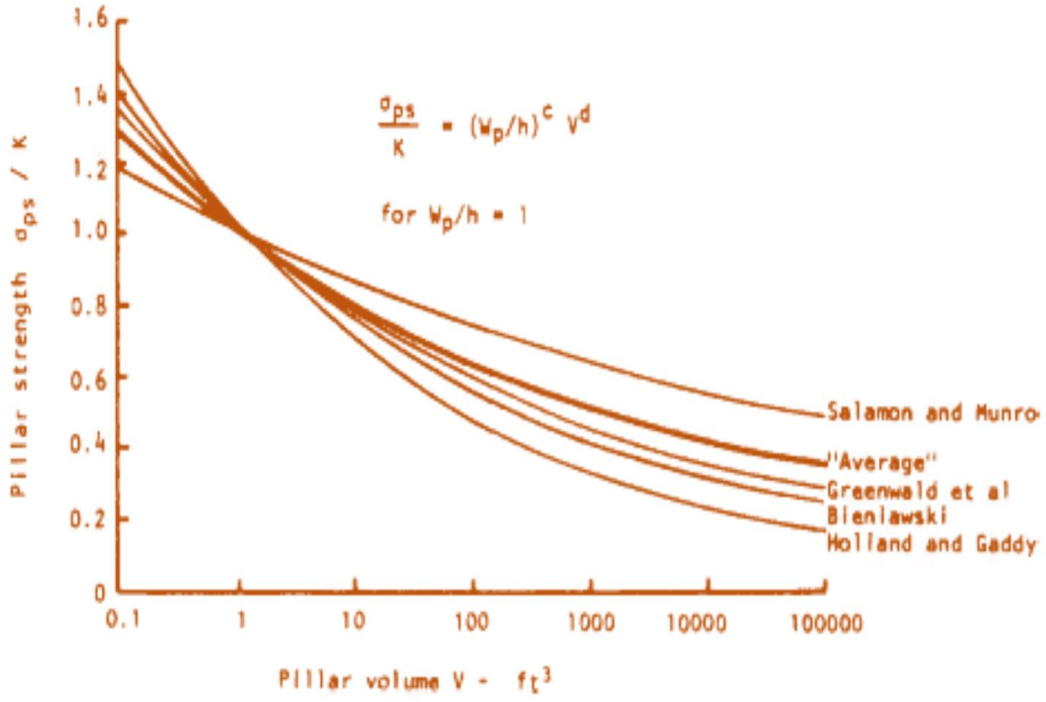

Figure 2.6. Relationship between pillar volume and pillar strength (Hoek and Brown,1980)

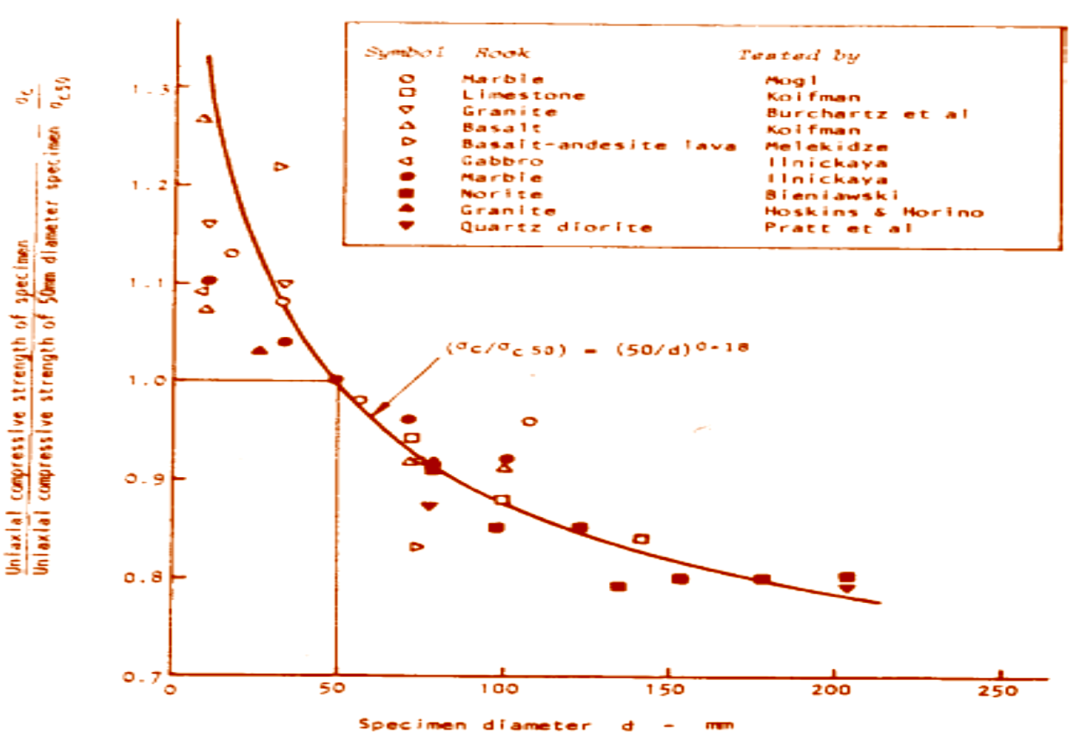

Figure 2.7: The effect of specimen size on intact rock strength (Hoek and Brown,1980).

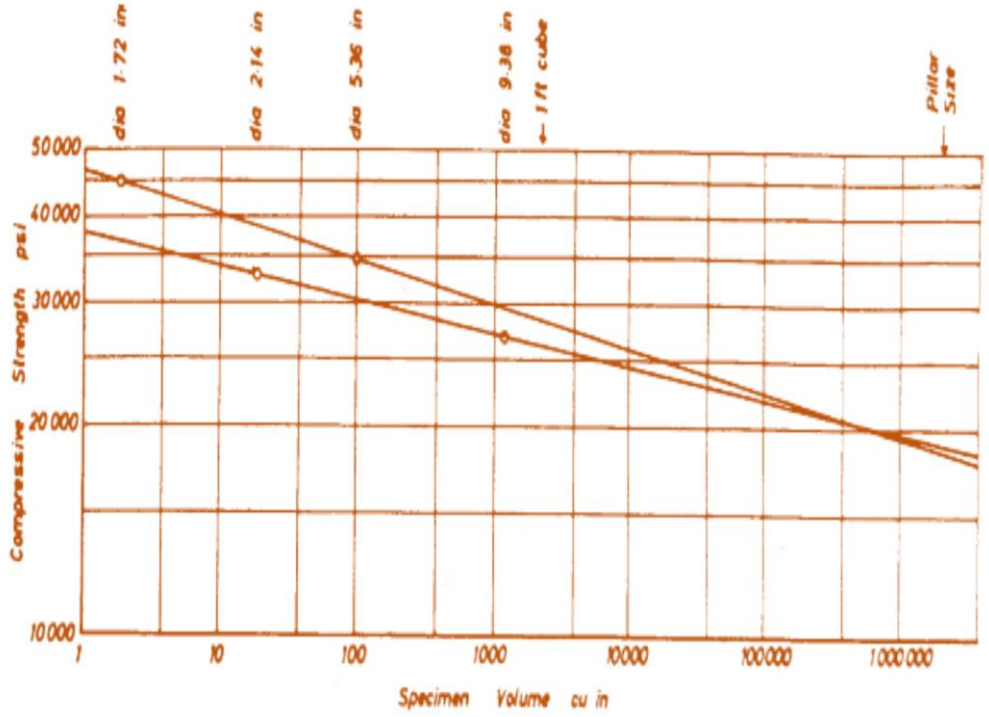

Figure 2.8: Compressive strength as a function of specimen size (Kostak,1971).

2.3.5 Pillar Modulus

The elastic modulus of a mine pillar represents the degree of fracturing as it is the main component of pillars elastic modulus. According to the work of John (1971), Hallbauer et al. (1973), Wagner (1974), the pillars elastic modulus does not started decreasing until 90-95 percent of the ultimate load of a sample has been reached. Figure 2.9 depicts a relationship proposed by Kostak and Bielenstein between pillar modulus and pillar size (1971).

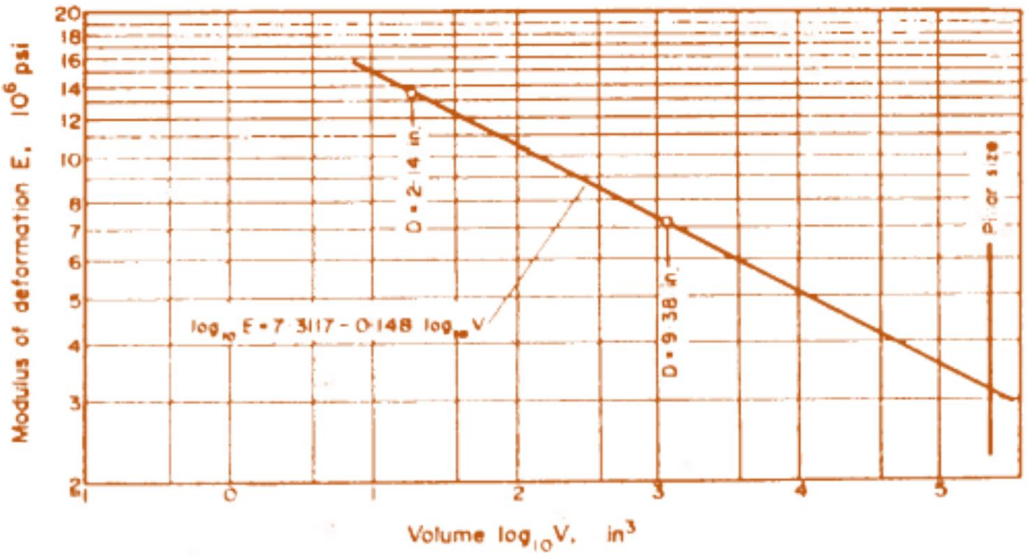

Figure 2.9: Size effect on modulus of deformation (Kostak and Bielenstien,1970)

2.3.6 Constitutive Relationship

The performance of the mine pillar under the load condition is determined by the constitutive relationship. Wagner's large-scale loading on a coal pillar has been depicted in Figure 2.10. (1974). According to the findings, the stress on the pillar has been more at the pillar core compared to the pillar perimeter. In failure situations, the core of the pillar is still stressed, and can be considered in the failure state. The variation in degrees of confinement with constitutive relationship has been illustrated in Figure 2.11. This variation demonstrates that the confinement increases, and also the pillar strength increases..

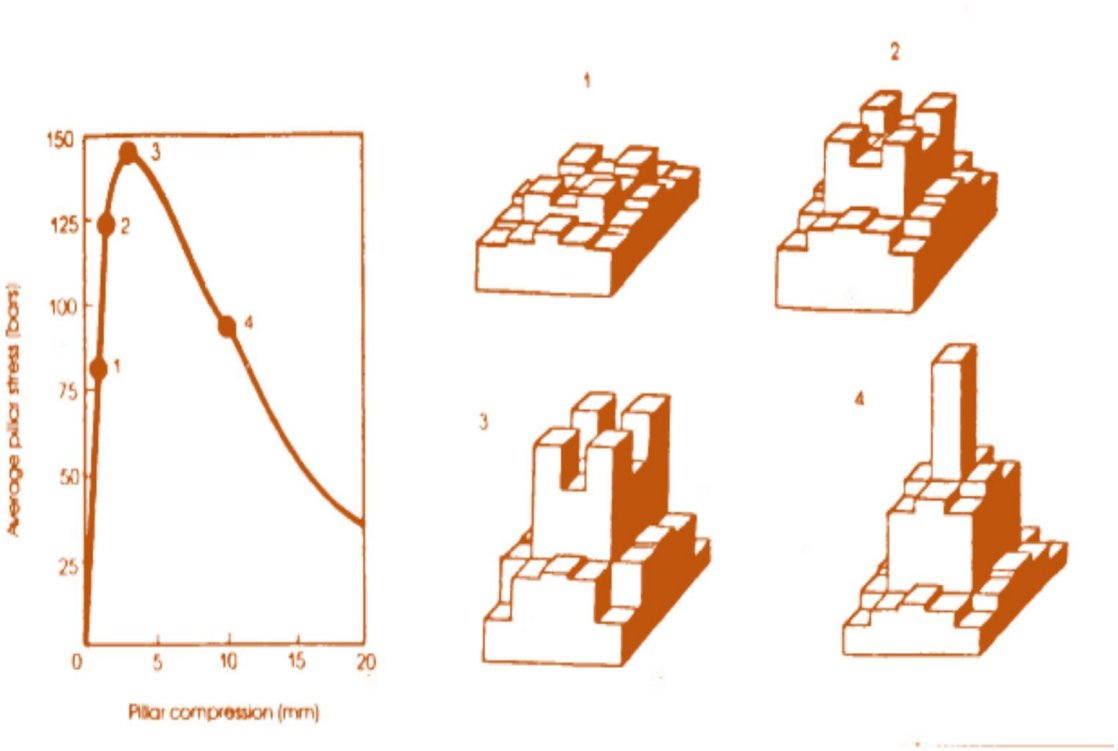

Figure 2.10: Stress distribution in coal pillar design at various stages (Wagner,1974).

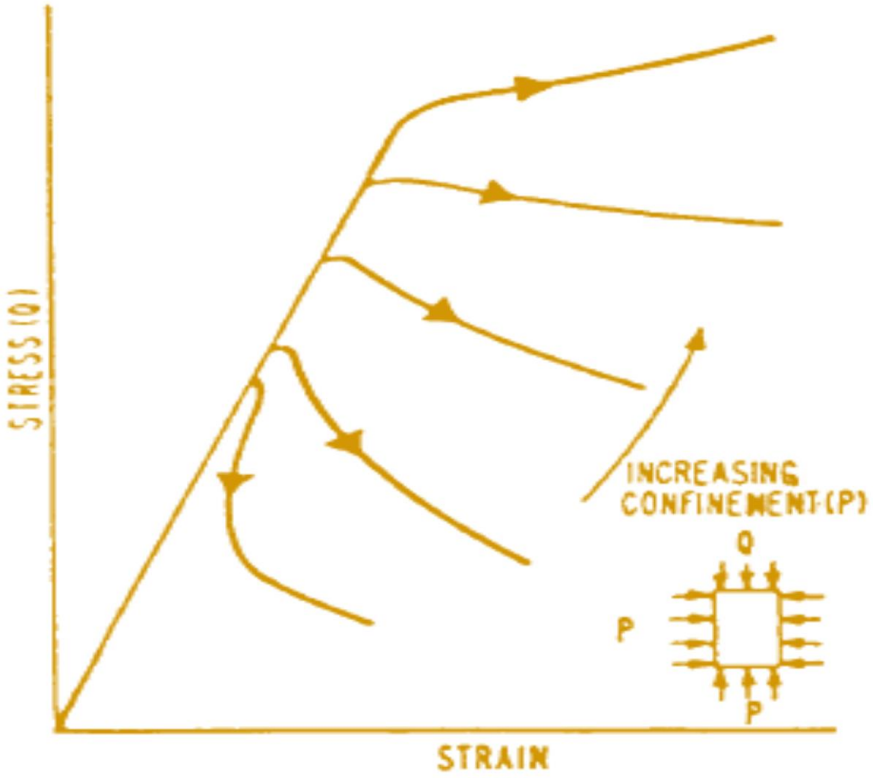

Figure 2.11: The stress-strain curve (Starfield and Faairhust, 1968

2.3.7 Pillar Confinement

Pillar confinement has been critical in defining strength and the type of failure. Square pillars may be weaker than rectangular pillars due to their lower average confinement. The w/h ratio has been commonly used as an input variable in determining the empirical strength formulae. However, this is only a significant predictor for pillar confinement.

2.4 Pillar Design Methodology

The purpose of pillars in mining is to keep adjacent strata stable for the duration of their expected lifespan. The primary, albeit simplified, form of the pillar strength equation has been represented in Equation 2.1. All strength formulae are based on the premise that a pillar fails when pillar stress exceeds pillar strength. However, the FoS has been used for compensating the error for the evaluation of the input parameters in the determination of the strength formulae.

$$\text{FoS} = \text{Pillar Strength} / \text{Pillar Stress} \tag{2.1}$$

Assessing pillar stress in non-tabular or irregularly dipping deposits is difficult to work to perform. By testing laboratory samples, the intact strength of a rock sample can be evaluated with adequate confidence. However, the correct method of assessing the strength of a full-size sample using this intact strength is complicated. Many researchers studying pillar strength have focused on acquiring the correlation between in-situ pillar strength and intact rock strength.

Using experiences under similar conditions is a common approach for pillar design. This method of trial and error may have some success from time to time, but it is not based on fundamental engineering principles. Pillar design is based on the premise that it is preferable in most cases to pillar design that will retain their overlying burden capacity all over their expected

lifespan. To accomplish the pillar design, it must be appropriate that the pillar strength must hold the capacity of overlying stresses. For designing the mine pillars the two crucial factors are pillar stress and pillar strength.

Because a rock mass is a heterogeneous and anisotropic medium, determining pillar strength is highly influenced by the factors that affect pillar strength, such as the structural features within the pillar, the pillar dimensions (w/h ratio, pillar height, and width of pillar), the intact strength of the pillar material, the material properties of the pillar, such as deformational characteristics, and the effects of blasting on the pillar.

Design techniques are primarily based on solving strength to stress in order to achieve a stable equilibrium. This necessitates making a stress estimate with the same level of precision as the strength estimates.The actual pillar stress has been influenced by in-situ stress conditions, the geographical locations of the mining area, the geological undulation such as faults, joints, unconformity, etc., the shape and dimensions of the pillars, the induced pillar load, and the groundwater.

The work of Potvin (1985) categorize pillar design into four major types:

1. Heuristic Method
2. Empirical, Method
3. Theoretical, Method
4. Computer Methods

These major classifications show the methods that have previously been used in pillar designing and assessing pillar strength. For the designing of mine pillars, Heuristic methods are most widely used and this method has been also considered as the most advanced method.

Accordingly, pillar design is mostly based on the premise that "what worked before could work again."

Empirical methods are based on experiments or personal experience. Various researchers have devised strength formulae for mine pillar design in their studies. The majority of the research was conducted in coal mines and extrapolated to hard rock underground mines.

Numerical methods have grown in popularity for evaluating stresses on pillars. Mine designs can be analyzed and pillar stresses predicted with the relatively affordable computing power accessible to rock mechanics engineers.

2.4.1 Pillar Stress Determination

Pillar stress is one of the difficult tasks to determine in underground mining. As previously mentioned, pillar stresses have been affected by a variety of factors, including mining-induced changes, in-situ stress conditions. In addition to it, pillar stress determination is also affected by geological features such as the shape and orientation of pillars, faults, and joints, groundwater, and spatial relation between pillars and mine openings.

Figure 2.12 is a simple representation of stress redistribution theory as a stream flow through bridge piers. The study describes two methods for evaluating pillar stress. These are two of them:

1. Tributary Area Theory.
2. Numerical Modeling Methods.

Tributary area theory is the most important and simple method of stress determination, whereas numerical modeling uses computational learnings in determining stress redistribution around mine openings. Further, the numerical modeling techniques are handled by the computers because complex nature of pillar stress.

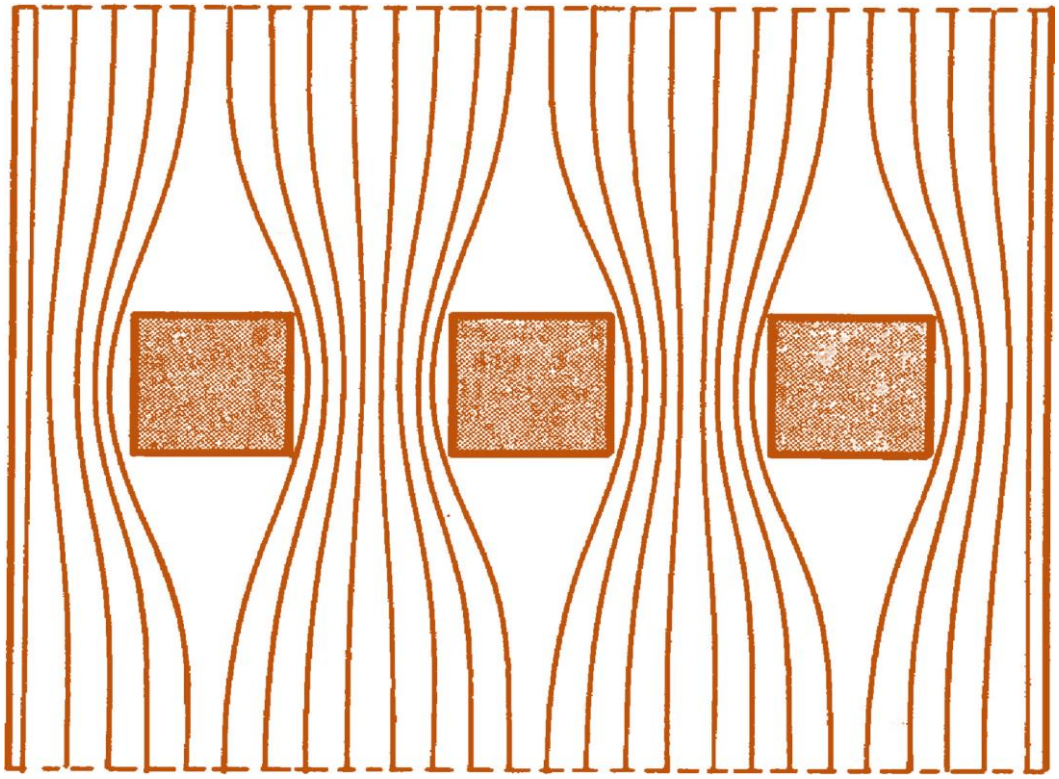

Figure 2.12. The streamlines in a smoothly flowing stream that is obstructed by three bridge piers are depicted (Hoek & Brown,1980).

The significance of accurately determining in-situ stresses cannot be overstated. The vertical in-situ stress component is commonly considered to be equal to the weight of the overburden lying on the strata. It might have been enough to determine the normal stresses acting on pillars in horizontally bedded deposits. However, in irregular, non-tabular deposits, all three principal stresses, not just the vertical component, influence the induced pillar stress. On average, in-situ stresses in a specific locality may not vary significantly. Still, they but they can vary considerably on a local scale due to geological structure and proximity to the surface. In-situ stresses have similar magnitudes and orientations over a large area (Herget,1987).

2.4.2 Tributary Area Theory

Tributary area theory was first introduced by Bunting in 1911 (Babcock et al. (1981)). The method is used to determine average pillar stress. Agapito (1972) represented that by using photo-elastic techniques in the study of stress analysis due to which tributary

area theory was originated. According to photoelastic studies, the applied load in pillars increased with increasing of slab openings and also the opening size to pillar size ratio. It was also shown as the number of openings increased to five or more, the applied load in the central pillars reached a maximum and became constant (Obert and Duvall, 1967).

As per tributary area theory, a pillar may very well sustain its "share" of the applied load. As a result, it is only applicable in this case, where comparable size pillars construct in a large continuous sequence, and it is unsuitable for irregular and dipping deposits, ambiguous or asymmetric mining patterns, and complex tri-axial stress fields.

Tributary area theory has proven most effective throughout horizontally bedded deposits that are homogeneous and also it covers a very large area, such as coal deposits or room and pillar mines. Equation 2.2 is the equation for tributary area theory in a room-and-pillar mine with equally sized rectangular pillars. Mining pillar layouts are depicted in Figures 2.13 and 2.14.

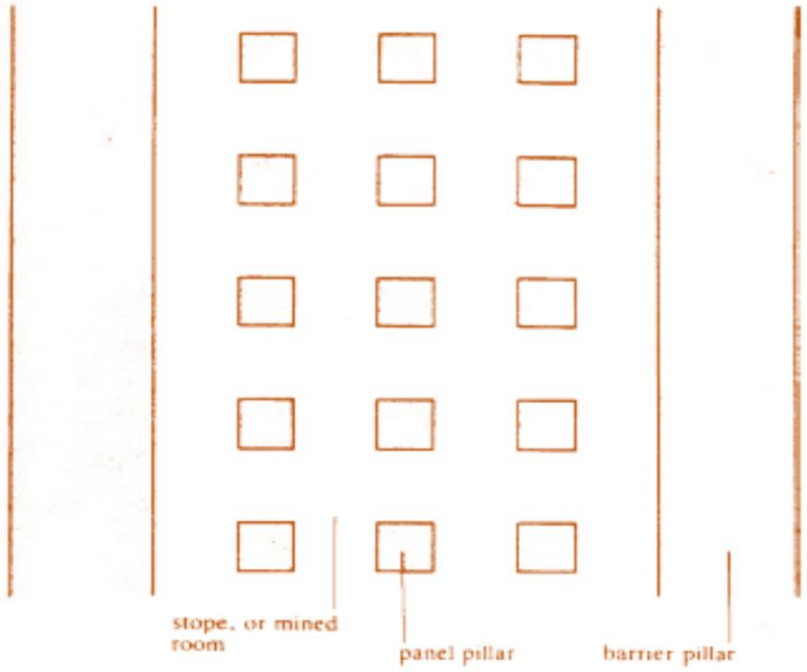

Figure 2.13 The configuration of barrier pillars and panel pillars in a horizontally extended ore (Brady and Brown,1985).

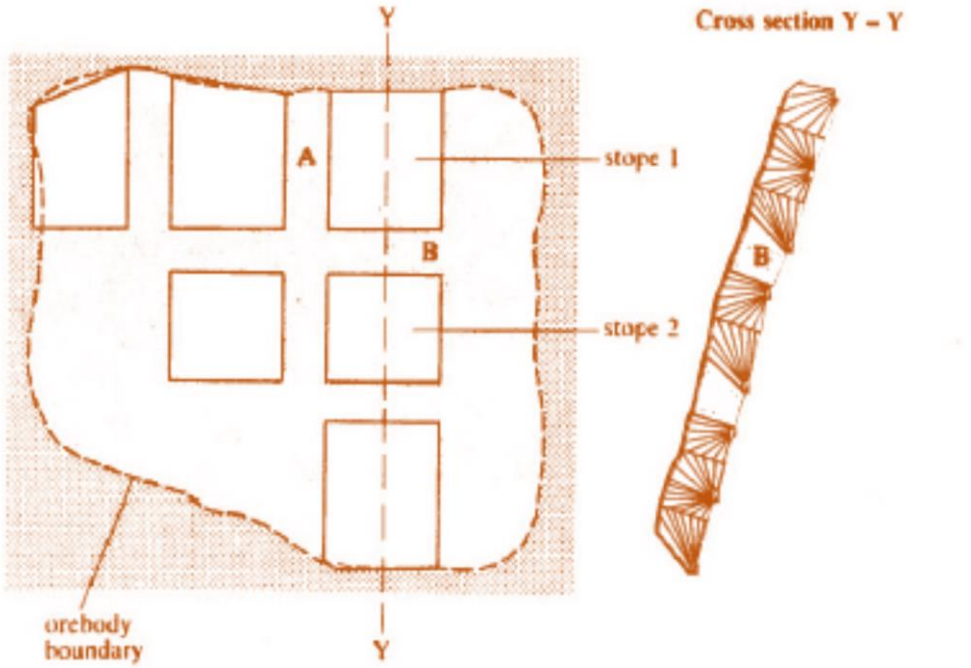

Figure 2.14 The pillar configuration for an inclined rock mass, with biaxially confined transverse and longitudinal pillars, 'A' and 'B,' respectively (Brady and Brown,1985).

$$\sigma_p = \gamma H.\left(1 + \frac{W_o}{W_p}\right).(1 + \frac{L_o}{L_p}) \qquad (2.2)$$

where:

σ_p	Pillar stress (MPa)
H	Depth of cover (m)
γ	Unit weight of rock (MN / m^3)
W.	Width (m)
L_o	Length (m)
Wp	Pillar width (m)
IP	Pillar length (m)

The extraction ratio formula is another name for tributary area theory. The amount of extraction around a set of pillars can be used to approximate the pillar's stress. Equation 2.3 expresses tributary area theory in this case.

$$\sigma_p = \frac{1}{1-R} \cdot \sigma_a \quad (2.3)$$

where:

R	Extraction Ratio
σ_p	Pillar stress (MPa)
σ_a	In-situ stress normal to mining horizon (MPa)

Tributary area theory has been used in tabular deposits where the stress normal to the orebody can be estimated with high confidence. This method has been frequently used in coal seams where overlying loads or stresses can be easily taken into account. Figures 2.15, 2.16, and 2.17 depicts the configuration of the pillars, and further the formulae which has been used to evaluate the pillar stress by using the tributary area theory. As previously stated, various forms of the tributary area theory have been presented for inclined mining configurations and triaxial stress conditions and these variation of tributary area theory are further discussed in the following sections.

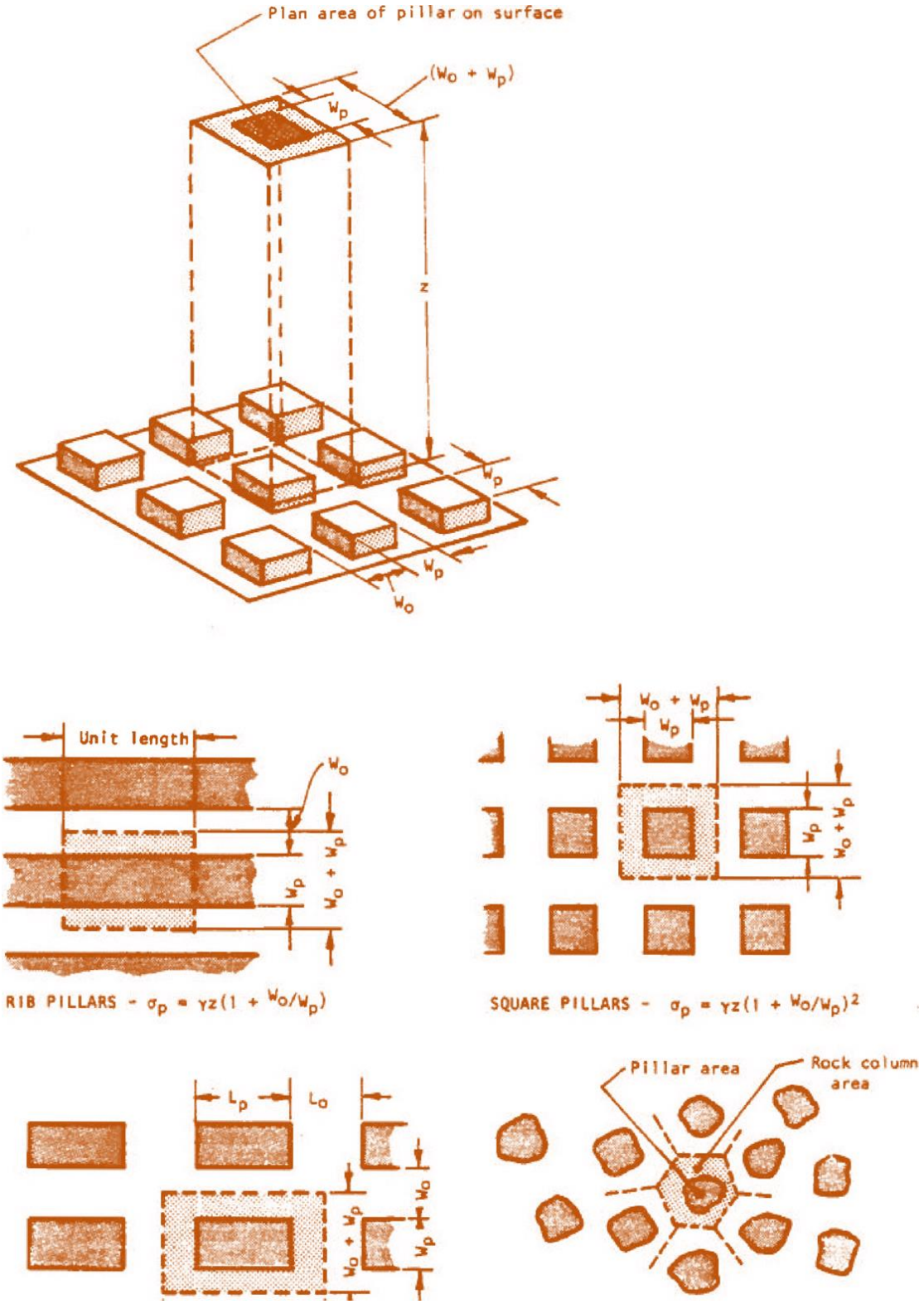

Figure 2.15: Loads are carried by various pillars in a typical pillar layout, assuming a total rock load evenly distributed across all pillars (Hoek & Brown, 1980).

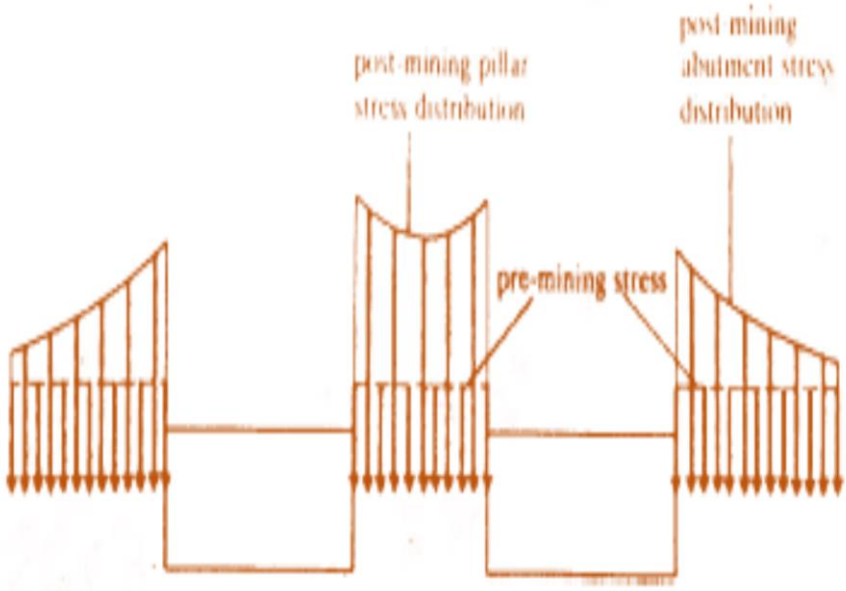

Figure 2.16: Stope development causes stress redistribution in the axial direction of a pillar (Brady & Brown, 1985).

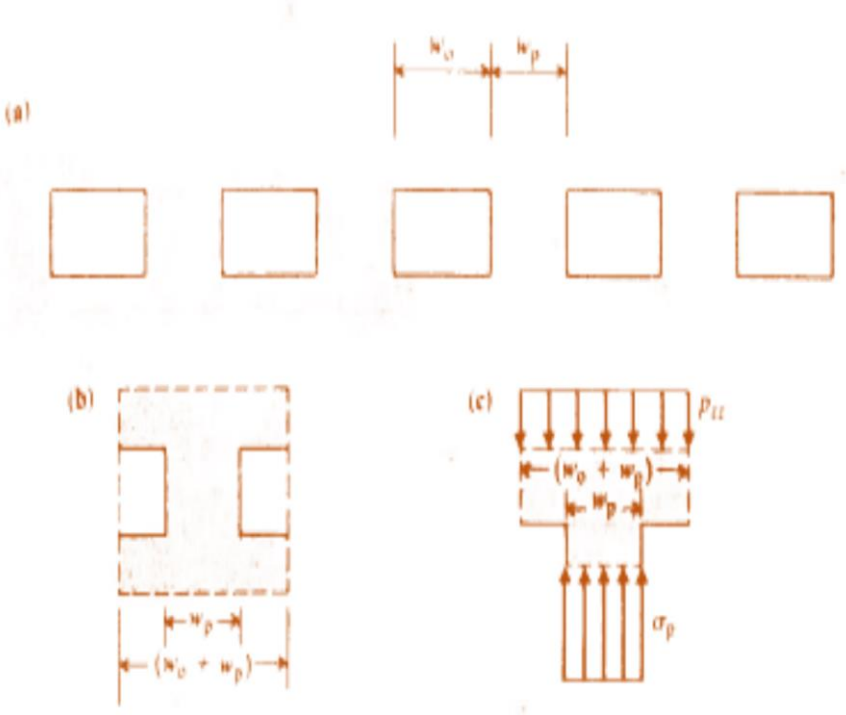

Figure 2.17: By utilizing long rooms and ribs pillars, the tributary area theory has been used to calculate the axial pillar stress in a large mine-structure (Brady and Brown,1985).

2.4.2.1 Inclined Stress Formula, Pariseau (1982)

For determining the stress acting on the pillars in the dipping seams which considered the both vertical and horizontal stress components into the account which is stated by (Pariseau (1982). The normal and shear stresses acting on inclined pillars are governed by Equations 2.4 and 2.5, respectively.

$$\sigma_p = \frac{\gamma H.(1+K_o)+\cos(2a)(1-K_o)}{2(1-R)} \quad (2.4)$$

$$\tau_p = \frac{\gamma H.\sin(2a).(1-K_o)}{2(1-R)} \quad (2.5)$$

where:

τ_p Shear pillar stress (MPa)

σ_p Normal pillar stress (MPa)

H Depth (m)

K_o Ratio of in-situ horizontal to vertical stress

γ Unit weight of overburden (MN / m^3)

R \Extraction ratio

α Dip (degrees)

This is an alteration to the tributary area theory approach for estimating normal, and shear stresses on a pillar while accounting for the tributary area theory approach for estimating normal and shear stresses on a pillar while accounting for both horizontal and vertical components of in-situ stress. The magnitudes of the horizontal stresses in the horizontal plane

are assumed to be equal. However, in general, horizontal stress magnitudes of horizontal stress can vary. Therefore, the above assumption is not always valid (Herget,1987).

2.4.2.2 Chain Pillar Formula, Szwilski (1982)

Szwilski (1982) modified the tributary area theory that was appropriate in longwall coal mines and it is also termed as Chain Pillar Formula. The formula for the stress estimation given a term that includes the additional load induced by the cantilevering effect of the excavated panel's immediate roof. Figure 2.18 depicts the terms used in the Chain Pillar Formula and the Chain Pillar Formula has been represented by equation 2.6.

$$\sigma_p = \gamma . H . \frac{(L_p+S)(W_f+2W_p+3S)}{2W_p L_p} \quad (2.6)$$

Where,

σ_p	Pillar stress (MPa)
H	Depth (m)
W_p	Pillar width (m)
L_p	Pillar length (m)
W_f	Width of the face (m)
γ	Unit weight of overburden (MN / m^3)
S	Spacing of chain pillars (m)

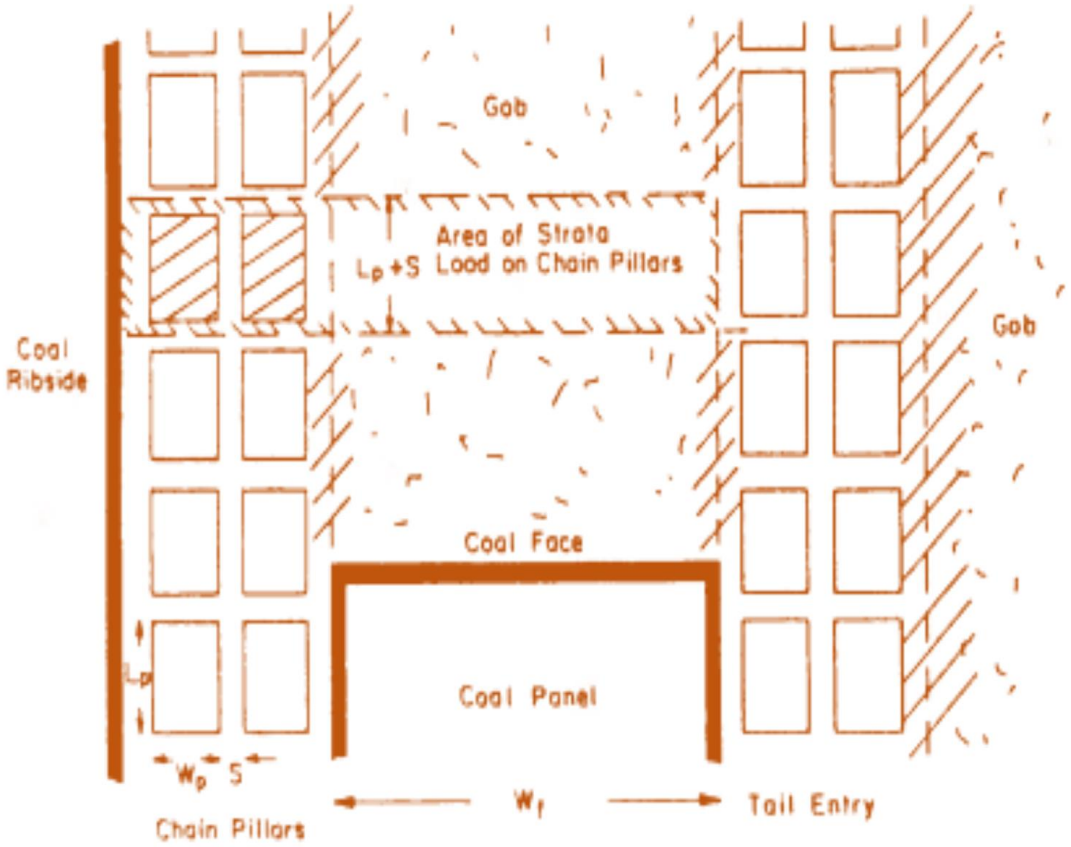

Figure 2.18. The "Chain Pillar Formula" layout (Szwilski, 1982).

2.4.2.3 Hedley & Grant Formula

Another extension of tributary area theory that reports for the inclined pillars geometry in a triaxial stress field has been proposed by Hedley & Grant (1972). This method takes into account the seam's dip as well as the vertical and average horizontal stresses exerting on the area under investigation. Equation 2.7 contains the Hedley and Grant stress formula for inclined pillars.

$$\sigma_p = \frac{\gamma H.cos2(a)+\sigma_h sin2(a)}{1-R} \qquad (2.7)$$

where

σ_p	Normal pillar stress (MPa)
H	Depth (m)
R	Extraction ratio
γ	Shear pillar stress (MPa)
α	Dip (degrees)
σ_h	The horizontal component of in-situ stress (MPa)

2.4.2.4 Subsidence Formula

Whittaker and Singh (1979) devised Equations 2.8 and 2.9 for evaluating stresses exerting on the barrier pillar in the longwall mining conditions. However, in this formula it has been assumed that the "goaf" area behind the longwall has been loaded by a triangular roof mass which has been sheared at an angle '$\boldsymbol{\phi}$', which has been measured from the vertical, near the rim of the barrier pillar. The load has been assumed to be transferred to the barrier pillars outside the triangular roof region.

$$\sigma_p = \frac{9.81\gamma}{1000w^2} \cdot \left\{\left[(W + w).H - \frac{w^2 cot\phi}{4}\right].w\right\} \quad (2.8)$$

for W/H < 2(tan$\boldsymbol{\phi}$)

$$\sigma_p = 9.81\gamma w \,.\, (w.H + H^2 tan\phi) \quad (2.9)$$

where:

σ_p	Pillar stress (MPa)
γ	Density (MN/m^3)
w	Width of barrier pillar(m)
H	Depth (m)
W	Width of longwall extraction
$\boldsymbol{\phi}$	Angle of shear of roof strata (degrees)

2.4.3 Numerical Modelling (methods)

Numerical modelling is the process of using numerical methods to solve problems involving the response of a rock mass to loading. Mining excavations, which cause a redistribution of stresses within the rock mass, are commonly responsible for loading. According to Brown (1987), "analytical solutions to practical rock mechanics problems are uncommon." This is due to the fact that simple mathematical functions cannot describe boundary problems associated with complex mining geometries. The governing equations are mostly nonlinear, the problem domain is heterogeneous and anisotropic, and the rock mass has no constitutive relations. The application of numerical models can be divided into two categories:

- It can be used in place of tributary area theory methods to determine pillar stress distributions. This method has been used when the conditions surrounding mining circumstances are so sophisticated that the tributary area method not be able to provide a relevant results for the calculations.
- Also, numerical methods are frequently applied for obtaining a proper pillar design. To analyze the predicted rock mass response, various modeling programs are used with failure criteria and strength parameters. Furthermore, failure analysis can be done interactively or as a post-processing routine. For determining pillar stresses, numerical modeling has specific advantages over tributary area theory. The elastic theory is commonly used in numerical modeling in order to estimate the stress redistribution within the domain of materials which has been differing in the elastic properties. Stresses can be estimated in complex mining geometries where tributary area theory formulae would not produce acceptable results. The use of numerical models, on the other hand, necessitates generalizations about the area of interest.

Among the numerical model programs some of the commonly used models in the mine design process are finite element models, distinct element models, finite difference models, fictitious force boundary element models, displacement discontinuity boundary element models, and hybrid models which are used as by combining two or more models for the designing of the pillars.

Determining pillar stresses in the given above methods requires knowledge of the pre-mining state of stress around excavations. Only the vertical stress acting on a seam in horizontally bedded deposits needs to be taken into account. This could be calculated by taking the products of the density of the overburdened rock mass by the depth of the cover beneath the surface. The overburden stress value is less reliable in hilly or mountainous areas, or in areas that have been glaciated. Without the use of in-situ measurement programs, it is very difficult to obtain the values of the in-situ stresses of the inclined orebodies. In their inclined stress formulae, Pariseau (1982) and Hedley & Grant (1972) both applied a terms that considered for the average in-situ horizontal stress. On the other hand, the horizontal components of in-situ stress are not always equal. As a result, the only method for accurately determining in-situ stress magnitudes has to put or take the in-situ stress measurements into the consideration. However, these tests have a very varying successful rate with a very high amount of cost (Pakalnis et al. 1985). It is clear from the above literature that several tests are necessary to be carried ot for obtaining reliable results. Furthermore, the obtained results are commonly used as the input data for all methods for calculating pillar stresses.

2.5. Pillar Strength Determination

Determination of the pillar strength is one of the important aspects of pillar design. To analyze pillar strength various studied has been proposed basically pillar strength determination methods can be categorized into:

- Empirical methods
- Theoretical methods
- Heuristic methods

In order to develop a strength formula which combines pillar stability and geotechnical terms, empirical methods has been used. For a given set of input parameters, mathematical methods are developed to determine the expected mine pillars' performance subjected to stress exerting on the pillars. Heuristic methods are "rule of thumb" methods for pillar design that ignore many of the valid pillar strength input parameters. In this section, the methods for estimating pillar strength proposed by various authors have been discussed.

2.5.1 Empirical Design Methods

Estimation of the pillar strength by empirical methods has been proposed by various researchers and brief studies for understanding the determination of pillar strength has been mentioned below:

- Linear Shape Effect Formula
- Power Shape Effect Formula
- Size Effect Formula
- Empirical Rock Mass Failure Criteria, Hoek & Brown,1980

The above results for evaluating the pillar strength are obtained by using pillar height, pillar width, UC,S and FoS as an input parameters. The width and height of a pillar are obtained by taking normal component and parallel component of the induced principal stress, respectively. All of the above mentioned formula have been represented by the Equation 2.10 but Hoek and Brown, (1980) found this equation by taking another considerations.

$$P_s = \left[a + b\left(\frac{w^A}{h^B}\right)\right] * K \quad (2.10)$$

where:

K	Strength of pillar material (Mpa)
P_s	Pillar strength (MPa)
h	Pillar height (m)
w	Pillar width (m)
A, B, a, b	Empirically constants

The generalized equation (2.10) has now been segregated into two well-known empirical methods, "Size Effect Formulae" and "Shape Effect Formulae." The Shape Effect Formula employs equal constants "a" and "b," indicating pillar strength does not have any affect due to pillar volume. The Size Effect Formula employs unequal constants "a" and "b," implying that the pillar strength decreases with an increase in pillar volume further for pillars having the same shape. Therefore the strength of the pillar reduces pillar volume increases. The same work has been reported by various researchers who, demonstrated that there is a decrease in pillar strength with increasing sample size. This is thought to be due to an increase in structural defects in larger sample specimens. Based on laboratory-sized specimens, Kostak and Bielenstein (1971) demonstrated that an increase in sample size resulted in a decrease in strength. With the exception of major structural features, Bieniawski and Denkhaus (1962) theree has no negative impact on pillar strength because their exist some critical sample size beyond the added structural defects with the exception of major structural features.

2.5.1.1 Linear Shape Effect Formula

Linear Shape Effect Formula presumes that pillars with equal w/h ratios will have equal strength regardless volume of pillars and the relation between pillar strength and w/h ratio will be linear. Equation (2.11) defines the Linear Shape Effect Formula.

$$P_s = \left[a + b\left(\frac{w}{h}\right)\right] * K \quad (2.11)$$

where:

K	Strength constant (MPa)
Ps	Pillar strength (MPa)
w	Pillar width (m)
h	Pillar height (m)
a, b	Empirically derived constants

2.5.1.1.1. Obert and Duvall (1967)

To estimate the col pillar strength based on the data of compressive strength performed on coal pillar specimens of different shapes (w/h ratios), Obert and Duvall (1967) has proposed Equation 2.12. In this formula, the strength term "K" refers to the pillar strength with a w/h ratio of one.

Table 2.2 illustrates the values of constants (A and B) obtained by various researchers for the above-given formula. Different studies performed of Obert and Duvall(1967), Bieniawski (1975), and Hudyma (1988) are presented in the following sections.

Table 2.2. **E**mpirical constants for Linear Shape Effect formula, "A" and "B", from various authors

Researchers	**A**	**B**	**w/h range**
Bunting (1911)	0.70	0.30	0.5-1.0
Obert & Duvall (1967)	0.78	0.22	0.5-2.0
Bieniawski (1968)	0.56	0.44	1.0-3.1
Van Heerden (1974)	0.70	0.29	1.1-3.4
Bieniawski (1975)	0.64	0.36	1.0-3.1
Sorenson & Pariseau (1978)	0.69	0.31	0.5-2.0

$$P_s = K.[0.222\left(\frac{w}{h}\right) + 0.778] \quad (2.12)$$

Where

Ps Pillar strength(Mpa)

K UCS(MPa)

w Pillar width(m)

h Pillar height(m)

According to Obert and Duvall (1967), when FoS lie between 2-4 then it has been used to determine size effect on strength.

2.5.1.1.2 Bieniawski (1975)

Bieniawski (1975) presented a Formula for the pillar strength of the coal pillars in the form of Equation 2.13 in which mentioned that the conclusion obtained has been given on tests which are performed on a large scale coal specimens. Furthermore, the given total number of tests performed by utilizing 66 samples whose length has been in the range of 0.6 – 2.0 meters in range and their w/h ratios were 0.5 – 3.4 in range. Moreover,(Bieniawski,1968) devised the Equation 2.13 by utilizing empirical constants of 0.556 and 0.444 in place of A and B.

$$P_s = K.[0.34\left(\frac{w}{h}\right) + 0.64] \quad (2.13)$$

where,

Ps Pillar strength(Mpa)

K UCS (MPa)

w Pillar width(m)

h Pillar height(m)

2.5.1.1.3 Hudyma (1988)

By using the compiled datasets from the Canadian hard rock underground mining operations Hudyma (1988) introduced the Pillar Stability Graph for evaluating the pillar strength of the open stope rib pillars . A number of 47 case histories of pillars sample has been collected in order to perform the work and also these sample are classified into stable pillars, slouging pillars and failed pillars. The statistical data, as well as predicted pillar loads, were used to create the Pillar Stability Graph. Based on pillar observations, three distinct regions were identified as failed cases, sloughing cases, or stable cases. Figure 2.19 depicts the pillar stability graph.

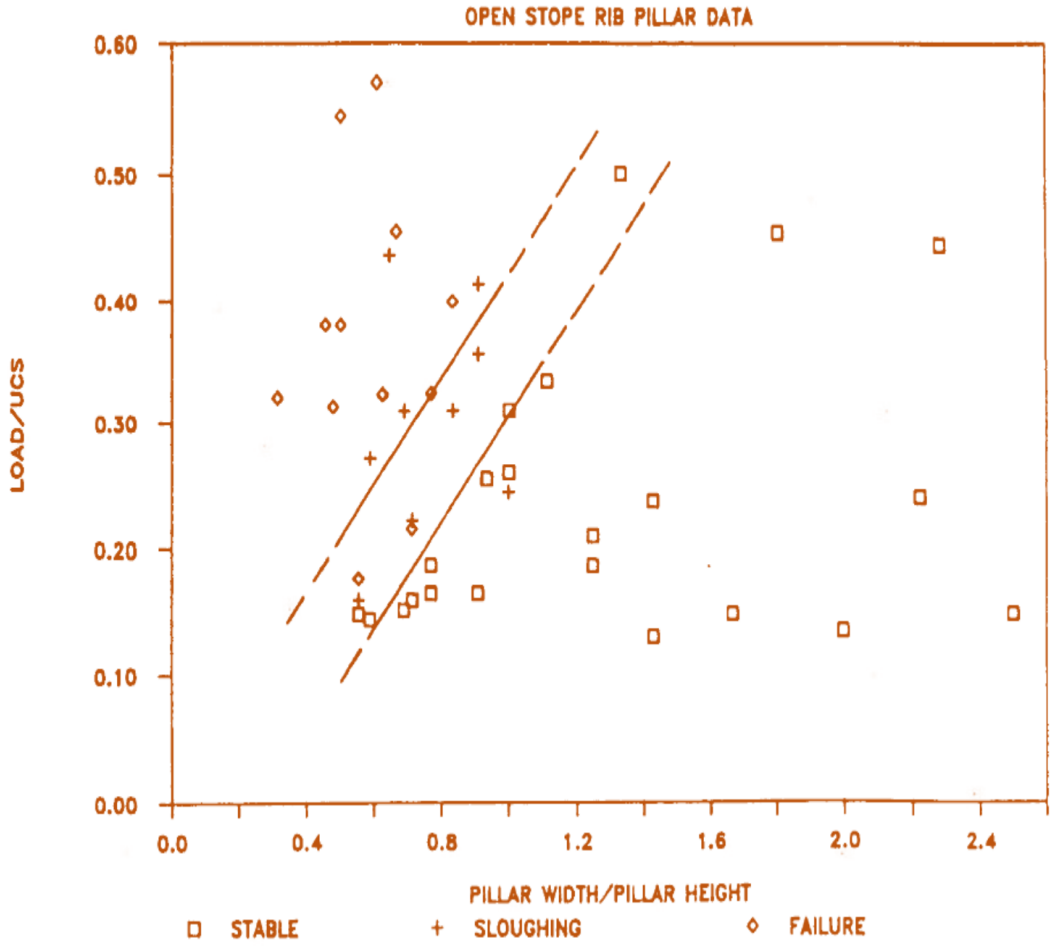

Figure 2.19. The pillar stability graph representing the stable, failed and transition zones (Hudyma 1988).

2.5.1.2 Power Shape Effect Formula

Power Shape Effect Formula has been proposed on the assumption that the strength of the pillar has been determined by using the square root of the pillar's w/h ratio. Equation 2.14 defines the formula. This relation was introduced by (Zern,1926; Holland,1956; Hazen & Artier,1976).

$$P_s = K * \sqrt{\frac{w}{h}} \tag{2.14}$$

Where,

Ps	Pillar strength(Mpa)
K	UCS (MPa)
w	Pillar width(m)
h	Pillar height(m)

2.5.1.3 Effective Pillar Width

The strengths of pillars with square plan cross-sections have been assessed in the majority of the cases listed in the preceding sections. Several authors have proposed that rectangular pillars will be stronger than square pillars due to increase in strength or in other words confinement from the pillar's long dimension in the plan. The suggested changes to the "Shape Effect Formula" to account for the increased confinement over a square pillar are listed below. In all cases, an effective pillar width term replaces the pillar width term in the strength formulae.

Sheorey and Singh (1974) suggested that the effective pillar width, taken into account as the average of the pillar's length and width, which could be replaced in place of the width in the shape effect formula. This study was performed on the testing of small-scale rectangular

specimens of varying sizes. Wagner (1980) and Stacey and Page (1986) both introduced a Equation 2.15 which could be used to replace the width of the pillar with the effective pillar width.

$$W_e = \frac{4.A_p}{R} \quad (2.15)$$

Where,

R Pillar circumference(m)

W_e Effective pillar width(m)

A_p Cross-sectional area of pillars(m)

These methods may be useful for extrapolating the strength of a square pillar to a rectangular pillar. The increase in strength that can be attributed to an increase in pillar side length, on the other hand, must have an upper limit. For very long pillars, the Wagner (1980) and Stacey and Page (1986) approaches to effective pillar width have upper limits of two times the minimum pillar width, whereas the Sheorey and Singh (1984) approach has an upper limit of one half the longer side of the pillar, making it the least conservative for strength estimation. Wagner's (1980) formula, according to Salamon (1983), provides an adequate estimate of the effective pillar width.

2.5.1.4 Hoek and Brown Failure Criteria

Hoek and Brown (1980) introduced a rock mass empirical strength criterion (Equation 2.16). According to the criteria, the influence of structural defects and pillar volume can be quantified by using rock mass classification parameters. These classifications yield empirical parameters "m" and "s" that are used to calculate the rock mass strength of a given rock. The estimated value was gathered to evaluate pillar stress, and a safety factor has been calculated. The empirical rock mass components "m" and "s"

values for various rock types and rock mass classification ratings are shown in Table 2.2 (Hoek & Brown, 1988). Figure 2.20 depicts the theoretical transformation of a rock mass from intact to extensively jointed condition.

$$\sigma_1 = \sigma_3\sqrt{[(m.\sigma_c\sigma_3) + (s.\sigma_c^2)]} \quad (2.16)$$

Where,

σ_1 Major principal stress(MPa)

σ_3 Minor principal stress (MPa)

σ_c UCS (MPa)

m, s Constants (Empirically derived).

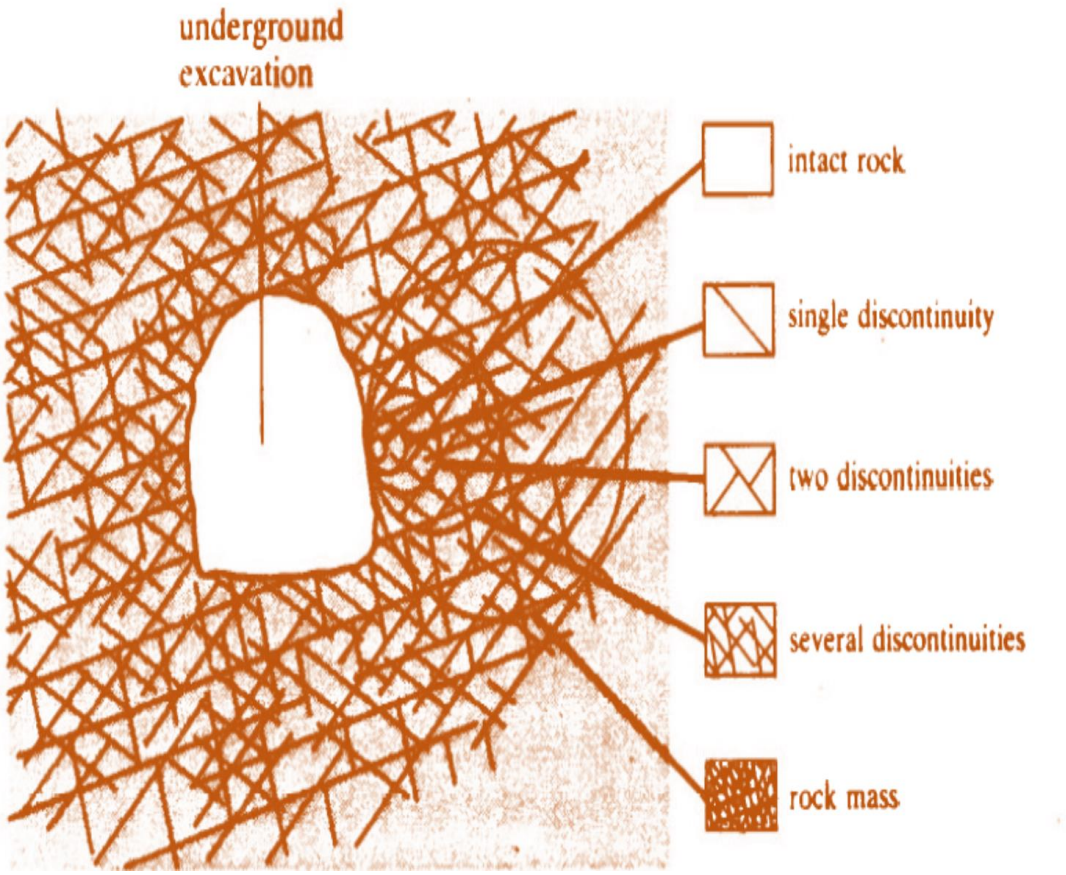

Figure 2.20. Idealized representation of the transition intact rock to bulky jointed rock mass with increasing sample size (Hoek & Brown, 1980).

Based on this strength criterion and the distribution of stresses inside modeled pillars, Hoek and Brown (1980) developed pillar strength curves. The pillar strength curves for igneous crystalline rock are plotted in Figure 2.21. The stress levels were calculated using two-dimensional boundary element modeling techniques. The failure of the pillar is assumed to occur when the factor of safety is less than one, based on the modelled stresses. Hoek and Brown (1980) proposed that the average pillar strength normalised to the unconfined compressive strength of intact pillar material could be determined for a given pillar width/height ratio and a rock mass rating.

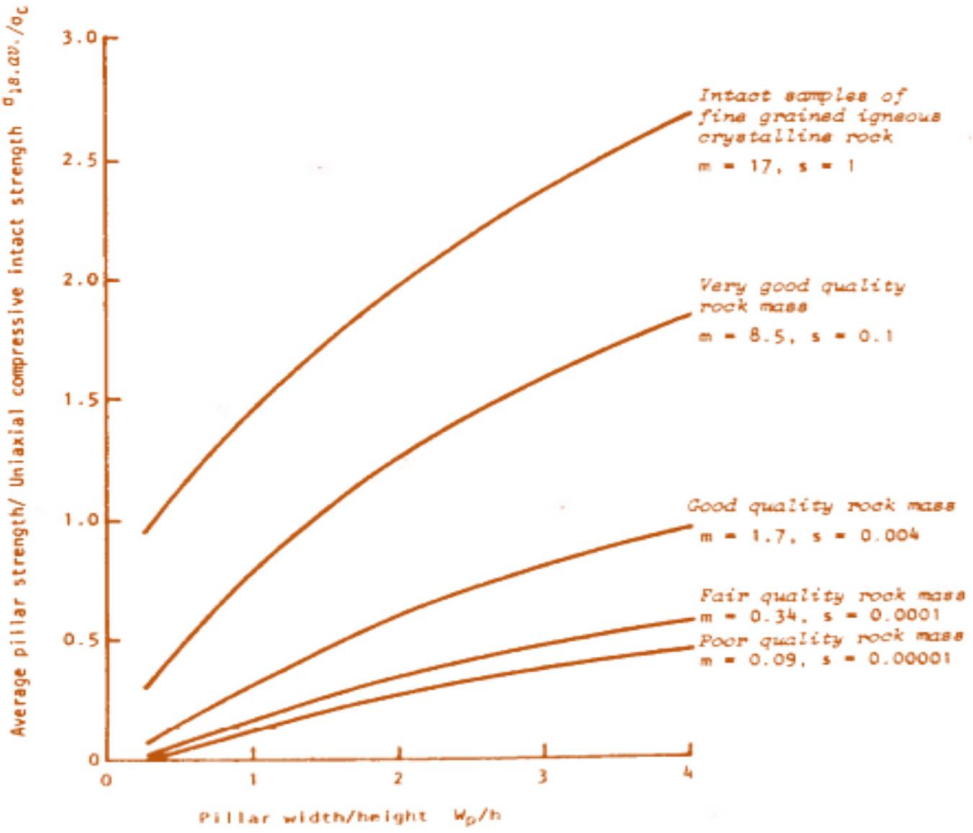

Figure 2.21: Pillar strength curves for crystalline igneous rock (Hoek & Brown, 1980).

2.5.1.5 The Size Effect Formula

A number of researchers have introduced empirical size effect strength formulae in the form of Equation 2.17. The formula given below has the effect that as dimensions of the pillar increase, the strength of pillars of similar shapes decreases.

$$P_s = \frac{w^a}{h^b} * K \quad (2.17)$$

Where,

K unconfined compressive strength (MPa)

Ps Pillar strength (Mpa)

h Pillar height(m)

w Pillar width(m)

a,b Constants (Empirical derived)

Various researchers have introduced the pillar strength formula in this form and the suggested values of the empirical constants are given in Table 2.3

Table 2.3**:** Empirical constants, "a" and "b", for Size effect formula given by different authors.

Authors	**a**	**b**
Greenwald et al. (1939)	0.5	0.833
Steart (1954)	0.5	1.0
Holland-Gaddy (1962)	0.5	1.0
Salamon and Munro (1967)	0.46	0.66
Bieniawski (1968)	0.16	0.55
Hedley and Grant (1972)	0.5	0.75
Sheorey et al. (1987)	0.5	0.86

2.5.1.5.1 Salamon and Munro Formula

Salamon and Munro (1967) investigated the strength of the pillars for square pillars in coal mines in South Africa. The database contained a total of 125 pillar cases which are further categorized into 98 pillar cases as stable cases and 27 pillar cases as failed cases, and its descriptions has been mentioned in Table 2.4. The tributary area method has been opted to calculate pillar stress acting on the pillar datasets. A descriptive statistical study has been

used for this data to obtain the empirical strength constants for the Size Effect Formula shown in Table 2.5. And also an important factor 'K' represented as coal strength constant which has been commonly used for the all the pillar case histories that has been denoted by Salamon and Munro , which was calculated statistically using all of the case histories in the database, with no context for the existing intact coal strength through each mining operation.

Salamon and Munro (1967) determined that the average FoS for the stable pillars is 1.6 whose diagrammatical representation in form of the histogram frequencies of pillars shown in Figure 2.22. In addition to it, Budavari (1983) concluded that most of the South African coal mines has adopted the Salamon and Munro formula having a FoS of 1.6 for the designing the pillar layouts.

Table 2.4**:** Description of the database for compiled case histories (Salamon & Munro, 1967)

Parameters	**Stable cases**	**Failed cases**
Number of Cases	98	27
Extration Ratio	37-89	45-91
Pillar Width (feet)	9-70	11-52
Pillar Height (feet)	4-16	5-18
Pillar Width / Height ratio	1.2-8.8	0.9-3.6
Depth (feet)	65-720	70-630

Table 2.5*:* Empirical constants obtained for size effect formula (Salamon & Munro, 1967)

K (strength, psi)	**A**	**b**
1322	0.66	0.46

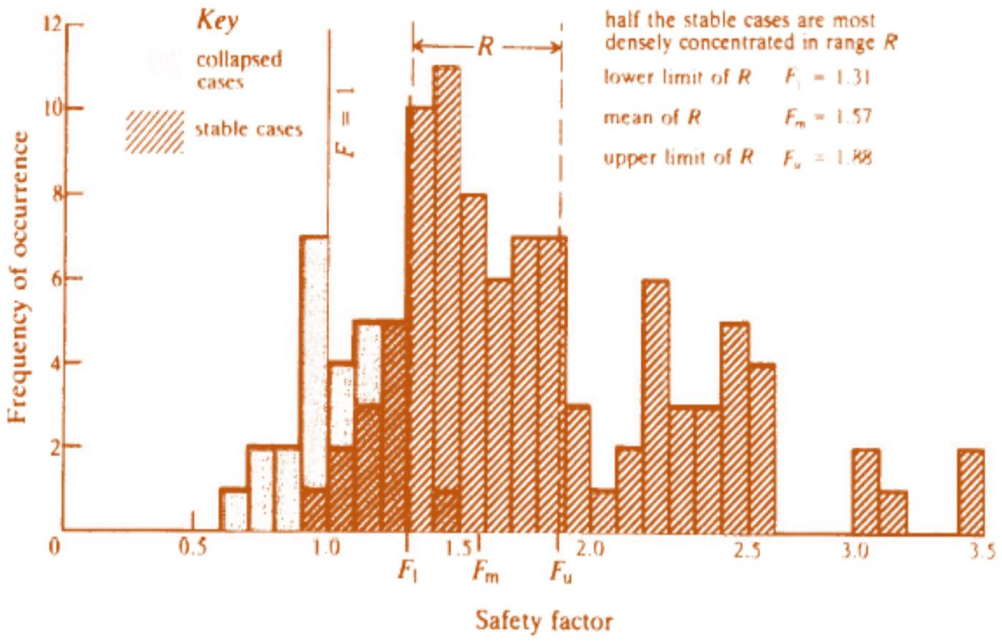

Figure 2.22: Histogram depicting the frequency of pillar performance and its failure shown for South African coal mines (Salamon and Munro, 1967).

2.5.1.5.2 Hedley and Grant Formula(1972)

Another variation of the pillar design method was introduced by Hedley and Grant (1972). The method proposed was totally composed of data acquired from uranium mines in the Elliot Lake district of Ontario, Canada. The study used a database containing 28 pillar case histories in which 23 stable pillars, two partially failed pillars, and three failed pillars). The study concludes that the pillar strength relationship could be approximated by a ″Size Effect Formula″ as shown in Equation 2.18.

$$P_s = K.\frac{w^{0.5}}{h^{0.75}} \tag{2.18}$$

Where,

K Strength of 30cm cubic sample (MPa)

Ps Pillar strength (Mpa)

h Pillar height(m)

w Pillar width(m)

The tributary area theory was used to calculate pillar stress, with modifications to account for the addition of horizontal in-situ stresses. The tributary area theory validation was done by taking Stress measurements by gathering in-situ of two mines. The authors concluded that the overall value of measured stress and tributary area theory has been comparably favorable, but there was a wide difference in the observed values. According to Hedley and Grant (1972), "the measurements themselves cannot be taken as accurately, and the results can vary by 50% uncertainty." This is the rare study in which one of the few times that hard rock pillar data has been used to develop a pillar strength formula.

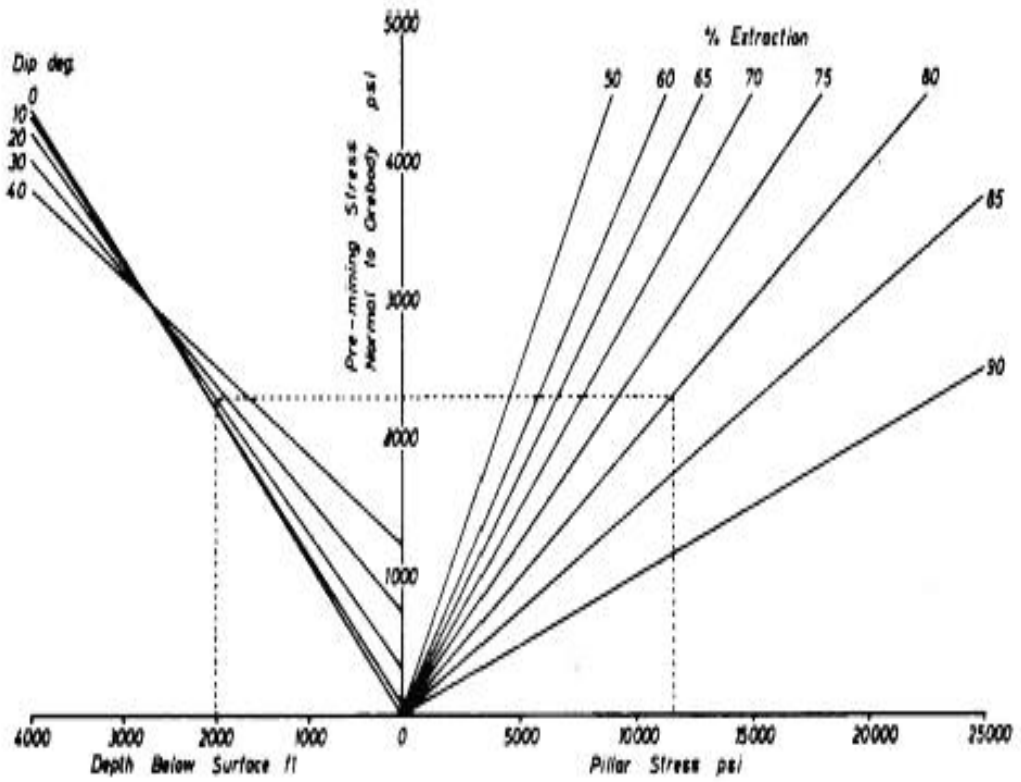

Figure 2.23 Pillar stresses obtained (Heddley and Grant, 1972)

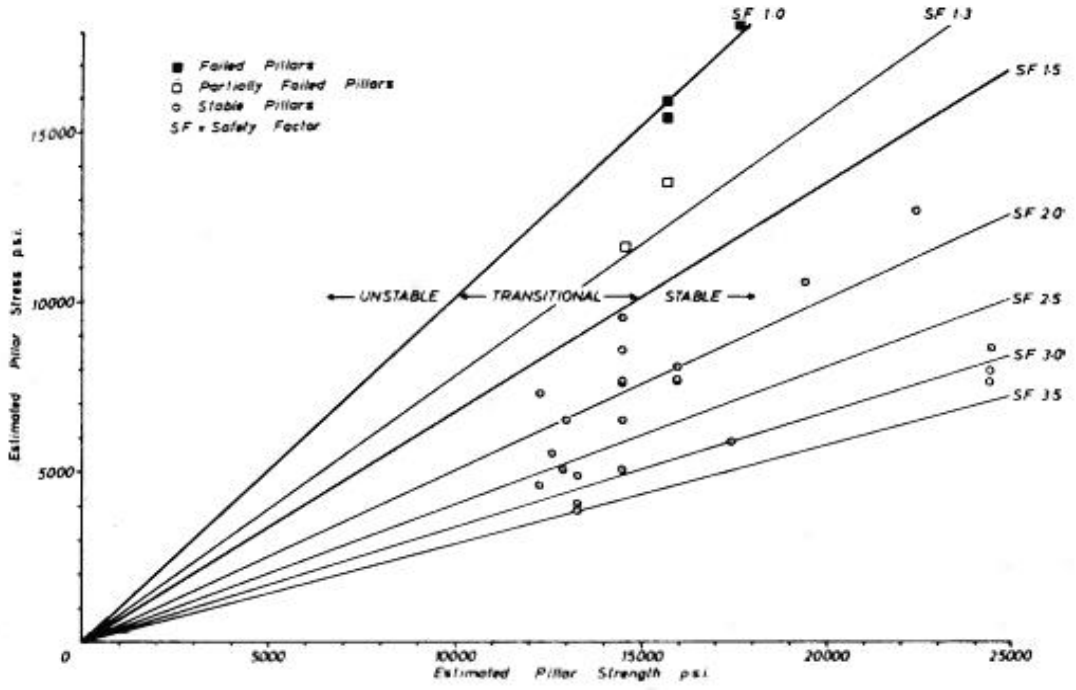

Figure 2.24**:** Pillar strengths and pillar stresses obtained by (Hedley & Grant, 1972).

1.5.1.5.3 Sheorey Formula

Another study was performed by Sheorey et al.(1987) on the coal mines in India. The empirical study of stable and failed pillars provides an empirical pillar strength formula presented in equation 2.19. In order to determine the strength formula 23 failed pillar cases and 20 stable pillar cases have been used. Further, they gave a slendor pillar's second strength formula in which pillar width to pillar height ratio is less than four as shown in equation 2.20.

In order to derive this formula stresses on the pillar were calculated by using the tributary area theory approach and moreover, numerical modeling was used to calculate the remaining pillar cases histories.

$$P_s = \frac{0.27\sigma_c}{h^{0.36}} + \frac{H}{160}.\left[\left(\frac{w}{h}\right) - 1\right] \quad (2.19)$$

$$P_s = 0.27\sigma_c.\frac{\sqrt{w}}{h^{0.86}} \quad (2.20)$$

Where,

K	Strength of 25 cm cubic sample (MPa, psi)
Ps	Pillar strength (Mpa, psi)
h	Pillar height(m)
H	Depth below the surface(m)
w	Pillar width(m)

The empirical strength formula is advantageous because it incorporates and observed full-size mine pillars for the study. However, they do not provide the mechanism of pillar loading and pillar failure, as well as no attempts, have been done. The following section investigates theoretical strength determination methods for mine pillars proposed by various researchers.

2.5.2 Theoretical Design Methods

The theoretical formula was also a well known method which has been designed by various number of researchers in which they has been used this method to determine the strength of the pillar mining areas. Also (Potvin,1985) has explained that the work of (Wilson's,1972) which has been discused in following section. In the work described by (Potvin,1985) it was stated that the combined core method is one of the single approach that has been used by Canadian mining operations in order to design the pillar.

2.5.2.1 Wilson Confined Core Method

According to mentioned work an attempt has been done to in order to calculate mathematically the initial features which has been influenced the whole strength of the pillars and also affected its design. To determine the pillar strength w/h ratio was takn to be more than 4.5 as governed by the Wilson confined core method. According to Wilson (1972), as

we move from pillar boundary to pillar core a transition has been observed in the yield zone(near pillar boundary) and progress into the undisturbed elastic zone (near pillar core). The relation has been defined by equation 2.21 and equation 2.22.

$$\frac{Y}{h} = \frac{1}{\sqrt{\tan(\beta).\tan(\beta-1)}}.\ln(\frac{\sigma_v}{\sigma_o}) \quad (2.21)$$

$$\tan(\beta) = 1 + \sin(\phi)\,/1 - \sin(\phi) \quad (2.22)$$

Where,

tan(**β**)	Triaxial stress coefficient
Y	Depth of yield zone
h	Seam height
$\boldsymbol{\phi}$	Angle of internal friction
$\sigma_{v.}$	Maximum pillar stress
σ_o	Unconfined compressive strength

Another work was done by Wilson (1972) in which he developed the formula for the pillar load which was basically relied upon the above theory given for wide pillars and slender pillars. Equation 2.23 has been used to define the slender pillar i.e. the criteria for the slender pillars. As the given requirement for the slender pillars is fulfilled then there would not be any confined pillar core and there will not be any elastic triaxial zone. The strength formula for the wide pillars and slender pillars are defined in equation 2.24 and equation 2.25 respectively. And Further, a similar type formula was also developed for the rectangular and long pillar by Wilson(1972).

$$w < 0.003.h*H \quad (2.23)$$

$$L = 4\rho * H(w^2 - 0.003 * w.h.H + 0.000003 * h^2H^2) \quad (2.24)$$

$$L = 444.\rho\frac{w^3}{h} \quad (2.25)$$

Where,

L	Pillar load(tons)
w	Pillar width(ft)
h	Pillar height(ft)
H	Depth(ft)
ρ	Density of rock(tons/ft^3)

2.5.2.2 Coates formula

Due to the increase in underground mining, the stress on the pillar walls increases, as a result the pillar walls deflected their from the original position. The work of Coates (1965) suggests the pillar load can be predicted by connecting the pillar walls' statically indeterminate deflection. The method was applicable in rib pillar mining with the involvement of ten measure variables and predict lower pillar stress than tributary area theory. Since the pillar wall deflection determination is difficult to measure the method seems to be impractical. To quantify the bending moment in the pillar wall, the pillar content must be intact and elastic in its behavior. However, because jointed rock masses break down continuously, acquiring the deflection measurement was found to be difficult. Moreover, (Agapito,1972) quoted that the approach of Coates and Ignatieff (1966) was difficult to verify in practice.

Many researchers have been derived the theoretical pillar strength formula but most of the formula are lacking in validation. However, the important feature of this theoretical work is that it may provide us with an overview of the mechanism of pillar loading and failure.

2.5.3. Heuristic Methods

Any approach to problem-solving or self-discovery that employs a practical method that is not guaranteed to be optimal, ideal, or rational, and something that is sufficient for reaching an instant, short-term purpose or approximation has been referred to as a heuristic technique.In past, few years lots of work has been done in pillar design based on the heuristic pillar design methods.

Thumb rule methods has been used to determine the strength formula and it was included in the the "Holland Formula" (Holland, 1964), "Mines Inspector Formula" (Ashley, 1930), the "Barrier Pillar Formula" (King and Whittaker, 1971) and Morrison et al. (1961) formula

2.5.3.1 Mines Inspector Formula

Equation 2.26 was introduced by Ashley (1930) in which Ashley (1930) has shown his work related to the Pennsylvania coal beds and also assumes that an arch approximately half the panel width will be stable. There is no verification that has been made to the materials of the pillar, density of the overburden, but it is quite fair to assume that the method has been intended to use only coal pillars. Equation 2.26 depicts the design of the pillars dimension. However, equation 2.26 does not use for the evaluation of the pillar strength.

$$w = H/10 + 4 * h + 20 \quad (2.26)$$

Where,

h Height of pillar(ft)

w Pillar width(ft)

H Depth of over(ft)

2.5.3.2. Holland Formula

The Holland formula is based on Belinski and Boreki's (1964) convergence research findings. In comparison to Ashley's formula, it gives a more accurate pillar width and takes into account pillar thickness as well as other persistent considerations. Holland's formula, on the other hand, is deficient in that it refuses to acknowledge the properties of the pillar rock. As a result, this method is only used in identical conditions to those in which the experiment was carried out. Equation 2.27 depicts another simplified method for pillar design in a coal mine.

$$w = 15\,T \quad or = \frac{1}{\mathrm{K}} * \frac{\log 2W_2}{\log(e)} \tag{2.27}$$

Where,

W_2 Estimated convergence(mm)

T The thickness of pillar (m)

w width of barrier pillar(m)

K Constant

2.5.3.3. Morrison Formula

The work of Morrison et.al (1961) was further reported by Potvin (1985). Based on mine safety research in Canada, the researchers examined an incredibly simplified formula for barrier pillar measurement, as shown by Equation 2.28. Basically, the Morrison formula only applies to abutment and barrier pillars. Besides this, his formula does not apply to rib and dip pillars.

$$w = \frac{1}{8} * D \ \ for\ D\ is\ less\ than\ 1200 \quad (2.28)$$

Where,

D Depth of cover (m)

w Pillar width(m)

2.5.3.4. Barrier pillar formula

King and Whittaker (1971) developed the thumb's rule approach for the design of barrier pillars again as shown in Equation 2.29. Furthermore, this formula has been deemed overly simplified and should only be used for rough calculations. This formula applies only to barrier pillars.

$$w = \frac{1}{10} * D + 45 \quad (2.29)$$

Where,

D Depth of cover (m)

w Width of the pillar(m)

2.6 Machine learning (ML)concept

ML is a branch of artificial intelligence aimed at programming and running machines**.** This is done using intelligent software that trains the model using inputs to achieve the desired results and reproduce the learning. The learning procedure can be supervised or unsupervised. In supervised learning, the records are labeled, i.e., the schooling samples comprise inputs with the corresponding output. In unsupervised learning, records are unlabeled, i.e., the schooling samples do not have a related output. In another variety of machine learning, the Semi-supervised learning works on an aggregate of labeled and unlabeled records while the reinforcement learning has no

records but only the set of rules to map conditions to moves to maximize a reward. A brief illustration of machine learning is given in Figure 2.25.

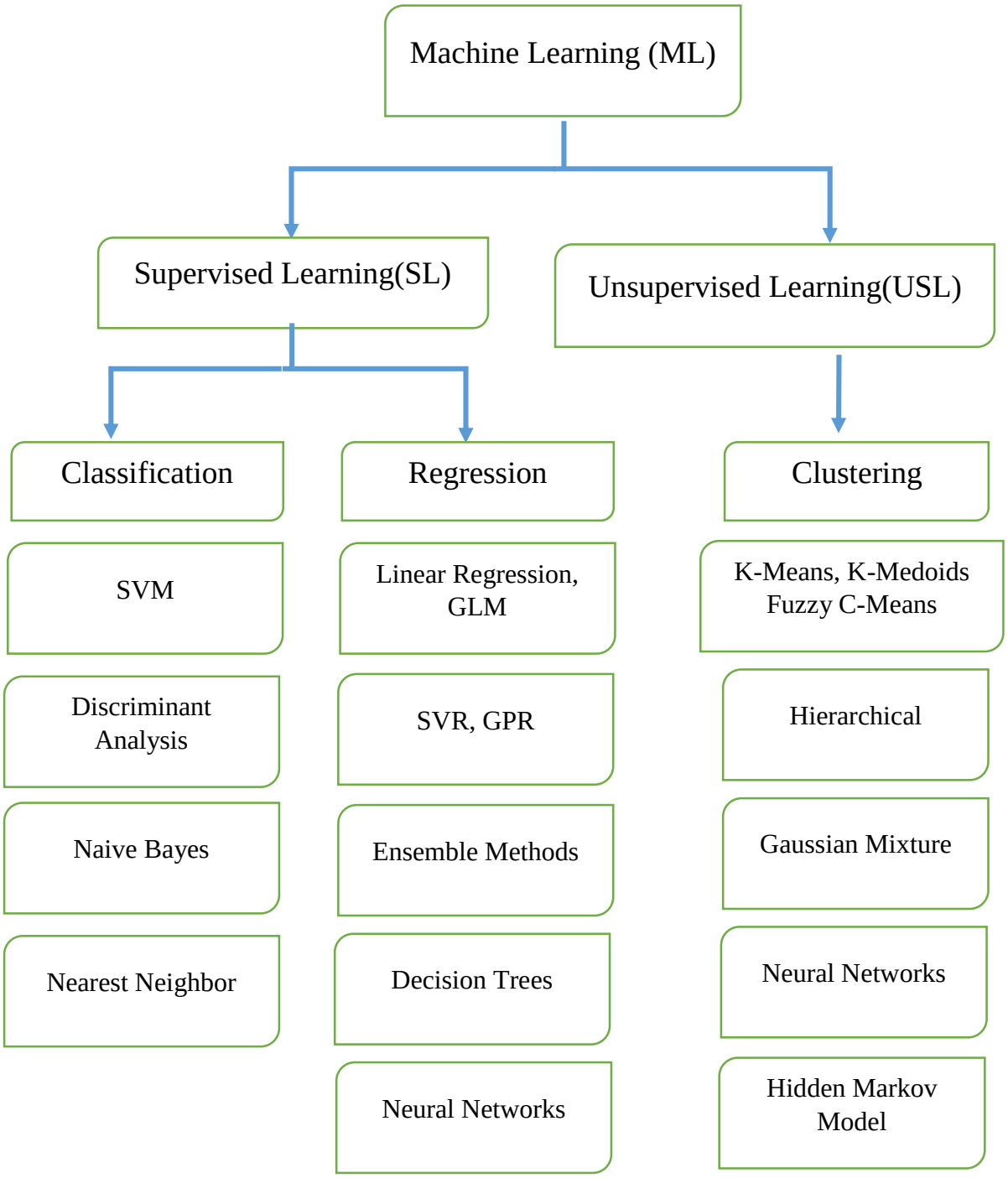

Figure 2.25. Introduction of machine learning.

ANN-based machine learning algorithms are broadly classified into categorical prediction models and numerical prediction models.

Categorical machine learning algorithms help in categorising data prediction**.** Decision Trees, SVM, Naïve Bayes Classification, k**-** Nearest Neighbors Classification, Random Forest are examples of categorical machine learning algorithms**.**

Numeric prediction models obtain a quote when enough information is not available to perform traditional calculations or relationships between input and output are too complicated for an analytical solution. Support Vector Clustering, k-Nearest Neighbors Regression, Artificial Neuron Network are typical numerical prediction tools.

Principal Component Analysis (PCA)

PCA is a widely used method to reduce the dimensionality of large data sets by altering a large set of variables into a smaller set that preserves the majority of the information in the larger set. Reduction in the number of variables in the data set leads to a reduction in the accuracy, but the trick to reducing size is to trade off a little precision for simplicity. The technique can be used on its own or as a data learning and data processing technique prior to another machine learning algorithm.

Smaller data sets are easier to explore and visualize, and they make data analysis for machine learning algorithms much easier and faster because there are no outliers to contend with.PCA is performed in the following steps :

- Ensure that the range of continuous initial variables seems to be uniform..
- Identification of correlations by computing the covariance matrix.

- In order to identify the principal components, computation of eigenvalue and eigenvectors of the covariance matrix are done.
- Creation of a feature vector to finalize which principal components to keep.
- Reframed the data along the axes of the principal components.

Multidimensional data should be visualized. Data visualizations, such as 2- or 3-dimensional plots, are an excellent tool for communicating multidimensional data. Condense information. PCA is used to compress data so that it can be stored and transmitted more productively. It can, for example, be used to compress images without compromising too much quality, or in signal processing. The technique has been successfully applied to a broad variety of compression problems, including pattern recognition (particularly face recognition), image recognition, and others.

PCA can be calculated in a variety of ways:

1. Covariance matrix Eigen decomposition
2. Data matrix singular value decomposition
3. Power iterative computation for eigenvalue approximation
4. Calculation of non-linear iterative partial least squares.
5.... and much more.

PCA has a number of advantages, but it also has some drawbacks.

PCA has the following advantages:

1. Simple to compute. PCA is based on linear algebra, which is computationally simple for computers to solve.

2. Accelerates other machine learning algorithms. When trained on principal components rather than the original dataset, machine learning algorithms converge faster.

3. Addresses the issues associated with high-dimensional data. Because of the high dimensionality of the data, regression-based algorithms easily overfit. We prevent the predictive algorithms from overfitting by using PCA beforehand to reduce the dimensions of the training dataset.

PCA has the following disadvantages:

1. Low interpretability of principal components. Principal components are linear combinations of the original data's features, but they are more difficult to interpret. For example, after computing principal components, it is difficult to determine which features in the dataset are the most important.

2. The relation made between information loss and reduced dimensionality while using the PCA has been described as dimensionality reduction is one of the important part which has been very much beneficial for the processing. The loss of information cannot be ignored and it is an unavoidable part of PCA.

Here are the assumptions and limitations made by the PCA

In Pearson correlation the description of PCA has been defined as the set of operations, so it inherits similar assumptions and limitations:

- PCA is totally based on the correlation properties of the parameters and also PCA will not be unable to estimate its principle components unless the parameters are not correlated..

- PCA is very active towards the range and domain of the parameters used. For example, let's have two features - one has values ranging between 0 and 1000, while the other has values ranging between 0 and 1 Regardless of the actual maximum variance in the data, PCA will be extremely biased towards the first feature being the first principle component. So its important to standardize values first.
- PCA is not invulnerable to outliers. As stated previously, the algorithm will be skewed in datasets with a high number of outliers. As a result, it is recommended that outliers be eliminated prior to conducting PCA.
- PCA assumes that features have a linear relationship. The algorithm is unsuitable for capturing non-linear relationships. As a result, it is recommended that non-linear features or relationships between features be converted to linear using standard methods such as log transforms.
- Technically applications generally assume that no missing data exist. When calculating PCA with statistical software tools, they frequently assume that the extracted parameters contain no missing data. End up making certain that any missing values from rows and/or columns are removed, or that missing values are imputed with a close approximation (e.g. the mean of the column).

Step-wise Selection and Elimination (SSE)

Step-wise Selection and Elimination (SSE) is a strategy that combines advancing and backward selection procedures. Stepwise regression is a forward adjustment of the determination in which all variables in the model are tested to see if their critical degree has been reduced below a predefined tolerance threshold after each progression in which a variable is included. If a variable is deemed to be non-significant, it is eliminated from the model. Stepwise regression has two levels: one for

adding variables and one for removing them. So that the procedure does not run into an unending circle, the limiting probability for adding variables differs from the limiting probability for removing variables. The following are the three sorts of techniques utilized in step-wise regression:

- Forward selection: It starts with no variables in the model and tests each one as it is introduced, then keeps those that are significant statistically, continuously repeating the process until the end.
- Backward elimination: It starts with the collection of independent variables, then begins with the removal of that variables one by one, and finally ensures or checks the variable which was removed is statistically significant or not.
- Bidirectional elimination: This is the combination of the first two procedures in order to determine which variables have to be included or excluded.